Chiral Organolanthanides Designed for Asymmetric Catalysis. A Kinetic and Mechanistic Study of Enantioselective Olefin Hydroamination/Cyclization and Hydrogenation by C_1-Symmetric $Me_2Si(Me_4C_5)(C_5H_3R^*)Ln$ Complexes where R* = Chiral Auxiliary

Michael A. Giardello, Vincent P. Conticello, Laurent Brard, Michel R. Gagné, and Tobin J. Marks*

Contribution from the Department of Chemistry, Northwestern University, Evanston, Illinois 60208-3113

Received February 17, 1994®

Abstract: The C_1-symmetric organolanthanide complexes $Me_2SiCp''(R^*Cp)LnE(SiMe_3)_2$ ($Cp'' = \eta^5$-Me_4C_5; R* = (1*S*,2*S*,5*R*)-*trans*-5-methyl-*cis*-2-(2-propyl)cyclohexyl ((+)-neomenthyl), (1*R*,2*S*,5*R*)-*cis*-5-methyl-*trans*-2-(2-propyl)-cyclohexyl ((–)-menthyl), and (1*R*,2*S*,5*R*)-*cis*-5-methyl-*trans*-2-(2-phenyl-2-propyl)-cyclohexyl ((–)-phenylmenthyl); Ln = La, Nd, Sm, Y, Lu; E = N, CH) serve as precatalysts for the efficient regio- and enantioselective hydroamination/cyclization of the amino olefins 1-aminopent-4-ene, 2-amino-hex-5-ene, 2,2-dimethyl-1-aminopent-5-ene, and 2,2-dimethyl-1-aminohex-5-ene to yield the corresponding heterocycles 2-methylpyrrolidine, 2,5-dimethylpyrrolidine, 2,4,4-trimethylpyrrolidine, and 2,5,5-trimethylpiperidine, respectively. At 25 °C, enantiomeric excesses as high as 69% (74% at –30 °C) and turnover frequencies as high as 93 h^{-1} are observed. Catalyst epimerization is observed in the presence of primary amines; however, equilibrium homochiralities are frequently very high (in some cases >95%), and epimerization is complete in the early stages of preparative scale reactions. The (+)-neomenthyl, (–)-menthyl, and (–)-phenylmenthyl catalysts afford 2-methylpyrrolidines with the (*R*) catalyst configuration selecting for (*R*) product configuration and (*S*) catalyst configuration selecting for (*S*) product configuration. Product stereochemistry can be understood in terms of olefin insertion via a chairlike, seven-membered transition state. The (+)-neomenthyl precatalysts (Ln = Nd, Sm) effect the cyclization of 2-aminohex-5-ene to *trans*-2,5-dimethylpyrrolidine in >95% diastereoselectivity at 25 °C. The corresponding hydrocarbyl complexes serve as precatalysts for the efficient asymmetric deuteration and hydrogenation of styrene and 2-phenyl-1-butene, respectively. For the organosamarium-derived catalysts, 2-phenyl-1-butene hydrogenation to yield exclusively 2-phenylbutane-1,2-d_2 under D_2 in a non-mass-transfer-limited reaction regime obeys the rate law $v = k[\text{olefin}]^0[\text{lanthanide}]^{1/2}[H_2]^1$, suggesting rapid, operationally irreversible olefin insertion (the step in which stereochemistry is fixed), a rapid preequilibrium involving an alkyl or alkyl/hydride dimer, and turnover-limiting hydrogenolysis of an intermediate samarium alkyl with k_{H_2}/k_{D_2} = 1.5–2.3 at 25 °C. Enantiomeric excesses as high as 64% (96% at –80 °C) and turnover frequencies as high as 26 000 h^{-1} are observed at 25 °C, P_{H_2} = 1 atm for the hydrogenation of 2-phenyl-1-butene. The (*R*) catalyst configuration selects for the (*R*) product and the (*S*) catalyst configuration for the (*S*) product, with no major nonlinear effects evident in studies with (*R*) + (*S*) mixtures. Product stereochemistry can be understood in terms of olefin approach along the ring centroid–metal–ring centroid angle bisector. Under the same conditions, the deuteration of styrene proceeds at comparable rates and higher selectivities, 72% (*S*) and 43% (*R*) ee with the (70/30) (*S*)/(*R*) and (*R*)-(–)-menthyl samarium hydrocarbyls, respectively. Exclusive formation of ethylbenzene-1,2-d_2 under D_2 indicates that β-hydride elimination/readdition does not effectively compete with turnover-limiting deuterolysis.

Introduction

In the preceding contribution,[1] we described the synthesis, characterization, configurational stability/dynamics, and stoichiometric reactivity of a new class of chiral, C_1-symmetric organolanthanide complexes of unambiguous absolute configuration. This contribution presents a full account of the scope and mechanism of two unusual asymmetric catalytic transformations mediated by these C_1-symmetric hydrocarbyls and amides (Scheme 1) numbering scheme of ref 1): one involving insertion of olefinic functionalities into d^0/f^n metal–amide bonds and the other involving reduction of olefinic functionalities at d^0/f^n centers incapable of oxidative addition–reductive elimination cycles and of forming conventional olefin π complexes. It will be seen that these organolanthanides serve as isolable, well-defined precatalysts for the asymmetric hydroamination/cyclization of amino olefins[2] and the asymmetric hydrogenation of styrenic olefins.[3] It is of interest here to compare and contrast reactivity and catalytic phenomenology of the new chiral organolanthanides with those of the well-characterized achiral Cp'_2LnR,[4-6] $Me_2SiCp''_2LnR$,[6a,7] and $R_2SiCp''CpLnR$[8] congeners ($Cp' = \eta^5$-Me_5C_5, $Cp'' = \eta^5$-

® Abstract published in *Advance ACS Abstracts*, September 1, 1994.

(1) Giardello, M. A.; Conticello, V. P.; Brard, L.; Sabat, M.; Rheingold, A.; Stern, C. L.; Marks, T. J. *J. Am. Chem. Soc.*, preceding paper in this issue.

(2) Communication of preliminary catalytic findings: Gagné, M. R.; Brard, L.; Conticello, V. P.; Giardello, M. A.; Stern, C.; Marks, T. J. *Organometallics* **1992**, *11*, 2003–2005.

(3) Communication of preliminary catalytic findings: Conticello, V. P.; Brard, L.; Giardello, M. A.; Tsuji, Y.; Sabat, M.; Stern, C.; Marks, T. J. *J. Am. Chem. Soc.* **1992**, *114*, 2761–2762.

(4) (a) Mauermann, H.; Marks, T. J. *Organometallics* **1985**, *4*, 200–202. (b) Jeske, G.; Lauke, H.; Mauermann, H.; Swepston, P. N.; Schumann, H.; Marks, T. J. *J. Am. Chem. Soc.* **1985**, *107*, 8091–8103. (c) den Haan, K. H.; de Boer, J. L.; Teuben, J. H.; Spek, A. L.; Kajic-Prodic, B.; Hays, G. R.; Huis, R. *Organometallics* **1986**, *5*, 1726–1733. (d) Watson, P. L.; Parshall, G. W. *Acc. Chem. Res.* **1985**, *18*, 51–55. (e) Heeres, H. J.; Renkema, J.; Booji, M.; Meetsma, A.; Teuben, J. *Organometallics* **1988**, *7*, 2495–2502.

(5) For studies of related Cp'_2ScR complexes, see: (a) Thompson, M. E.; Bercaw, J. E. *Pure Appl. Chem.* **1984**, *56*, 1–11. (b) Burger, B. J.; Thompson, M. E.; Cotter, D. W.; Bercaw, J. E. *J. Am. Chem. Soc.* **1990**, *112*, 1566–1577.

0002-7863/94/1516-10241$04.50/0 © 1994 American Chemical Society

Scheme 1. Chiral Organolanthanide Hydrocarbyl and Amide Precatalysts

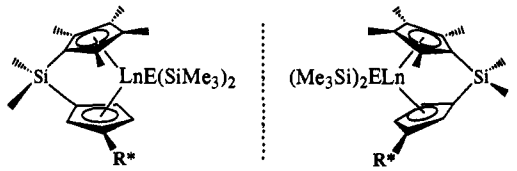

(S) (R)

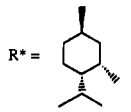

R* = (+)-neomenthyl

E = CH, Ln = La (**6a**), Nd (**6b**), Sm (**6c**), Y (**6d**), Lu (**6e**)
E = N, Ln = La (**7a**), Sm (**7b**), Y (**7c**), Lu (**7d**)

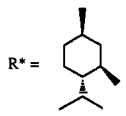

R* = (-)-menthyl

E = CH, Ln = Sm (**6f**), Y (**6g**), Lu (**6h**)
E = N, Ln = Sm (**7e**), Y (**7f**), Lu (**7g**)

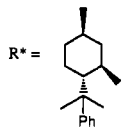

R* = (-)-phenylmenthyl

E = CH, Ln = Y (**6i**)
E = N, Ln = Y (**7h**)

Me_4C_5; R = $E(SiMe_3)_2$; E = CH, N). For example, the present chiral hydrocarbyl and amide complexes offer a level of ring substitution/coordinative unsaturation intermediate between known $Me_2SiCp''_2LnR$ and $R_2SiCp''CpLnR$ structures. Previous studies showed that in the increasingly unsaturated series Cp'_2LuR, $Me_2SiCp''_2LuR$, and $Et_2SiCp''CpLuR$ (R = $CH(SiMe_3)_2$), a rate increase of >200× is observed for the hydroamination/cyclization of 2,2-dimethyl-1-aminopent-4-ene to 2,4,4-trimethylpyrrolidine at 80 °C (eq 1).[9] Conversely, for 1-hexene hydro-

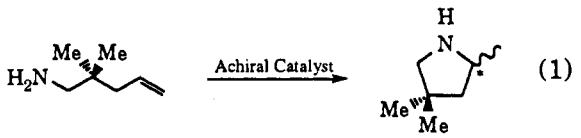

(1)

genation, the Cp'_2Lu-based catalyst[6a] exhibits a turnover frequency in excess of 120 000 h^{-1} at 25 °C, 1 atm of H_2 pressure, while the $Et_2SiCp''CpLu$-based catalyst exhibits a turnover frequency of <25 h^{-1} under identical conditions.[8] The latter hydride also undergoes an unusual ligand redistribution reaction to a "spanning" $Lu_2(\mu\text{-}Cp''SiEt_2Cp)_2$ structure which renders it incompetent for catalytic olefin hydrogenation (**A**).[8]

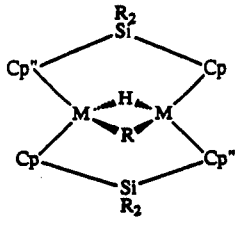

A

For efficient chirality transfer in catalytic asymmetric olefin hydroamination and hydrogenation at a lanthanide center, the stereodifferentiating step in the catalytic cycle would seem to require operationally irreversible olefin insertion into a Ln–N or an Ln–H bond, respectively, followed by rapid, stereospecific Ln–C scission to yield product. The asymmetrically configured disposition of the present ligation, as characterized by solution spectroscopy and single crystal X-ray diffraction,[1] has been designed to enhance stereofacial selection in the approach of prochiral olefinic substrates to the highly electrophilic lanthanide center. The nature and tunability of these substrate–catalyst interactions serve as the basis for the present kinetic/mechanistic analysis of asymmetric induction and convey significant implications for designing analogous transition metal-based catalysts as well as for further ligand engineering.

Experimental Section

Materials and Methods. All manipulations of air-sensitive materials were performed with rigorous exclusion of oxygen and moisture in flamed Schlenk-type glassware on a dual manifold Schlenk line or interfaced to a high-vacuum (10^{-6} Torr) line or in a nitrogen-filled Vacuum Atmospheres glovebox with a high-capacity recirculator (1–2 ppm of O_2). Argon (Matheson, prepurified), dihydrogen (Linde), and deuterium (Isotec) were purified by passage through a MnO oxygen-removal column[10] and a Davison 4 Å molecular sieve column. Hydrogen and deuterium for catalytic hydrogenation kinetic studies were purified additionally via passage through a freshly activated column of MnO/silica[10] positioned immediately before the reaction vessel. Ether solvents were distilled under nitrogen from sodium benzophenone ketyl. Hydrocarbon solvents (toluene, pentane, and heptane) were distilled under nitrogen from Na/K alloy. All solvents for vacuum line manipulations were stored *in vacuo* over Na/K alloy in resealable bulbs. Deuterated solvents were obtained from Cambridge Isotope Laboratories (all 99+ atom % D) and were degassed and dried over Na/K alloy. Toluene-d_8 for kinetic measurements was stored *in vacuo* over Na/K alloy and was vacuum-transferred immediately prior to use. The prochiral olefin 2-phenyl-1-butene was prepared[11] from propiophenone via Wittig reaction with methylenetriphenylphosphorane and was degassed, dried over Na/K alloy for 0.5 h, and vacuum-transferred prior to use. Styrene (Aldrich, Gold Label) was washed with base, distilled twice from CaH_2, and vacuum-transferred from activated alumina immediately prior to use. The prochiral amino olefins, 1-aminopent-4-ene, 2-aminohex-5-ene, 2,2-dimethyl-1-aminopent-4-ene, and 2,2-dimethyl-1-aminohex-5-ene,[12] were prepared according to methods developed in this laboratory,[9c] predried over KOH, freeze–pump–thaw degassed, and vacuum-distilled from Na/K alloy. (*S*)-(+)-2-Phenylbutanol was prepared according to literature procedure.[13]

Physical and Analytical Measurements. NMR spectra were recorded on either Varian VXR 300 (FT, 300 MHz, ^1H; 75 MHz, ^{13}C) or XL-400 (FT, 400 MHz, ^1H; 100 MHz, ^{13}C) instruments. Chemical shifts for ^1H, ^{13}C NMR are referenced to internal solvent resonances and are reported relative to TMS. NMR experiments on air-sensitive samples were conducted in either Teflon valve-sealed tubes (J. Young) or in screw-capped tubes fitted with septa (Wilmad). Optical rotations were measured at 26 °C with an Optical Activity Ltd. AA-100 polarimeter (±0.001°) using a 0.5 dm quartz cell. Concentrations reported with specific rotations are in units of g·(100 cm^2)$^{-1}$. Analytical gas chromatography was performed on Varian Model 3700 gas chromatograph with FID detectors and a Hewlett-Packard 3390A digital recorder/integrator using a 0.125 in. i.d. column with 3.8% w/w SE-30 liquid phase on Chromosorb W

(6) (a) Jeske, G.; Lauke, H.; Mauermann, H.; Schumann, H.; Marks, T. J. *J. Am. Chem. Soc.* **1985**, *107*, 8111–8118. (b) Evans, W. J.; Bloom, I.; Hunter, W. E.; Atwood, J. L. *J. Am. Chem. Soc.* **1983**, *105*, 1401–1403.

(7) (a) Jeske, G.; Schock, L. E.; Swepston, P. N.; Schumann, H.; Marks, T. J. *J. Am. Chem. Soc.* **1985**, *107*, 8103–8110. (b) Heeres, H. Ph.D. Thesis, University of Gröningen, Gröningen, the Netherlands, 1990.

(8) Stern, D.; Sabat, M.; Marks, T. J. *J. Am. Chem. Soc.* **1990**, *112*, 9558–9575.

(9) (a) Gagné, M. R.; Marks, T. J. *J. Am. Chem. Soc.* **1989**, *111*, 4108–4109. (b) Gagné, M. R.; Nolan, S. P.; Marks, T. J. *Organometallics* **1990**, *9*, 1716–1718. (c) Gagné, M. R.; Stern, C.; Marks, T. J. *J. Am. Chem. Soc.* **1992**, *114*, 275–294.

(10) (a) Moeseler, R.; Horvath, B.; Lindenau, D.; Horvath, E. G.; Krauss, H. L. *Z. Naturforsch.* **1976**, *31B*, 892–893. (b) McIlwrick, C. R.; Phillips, C. S. G. *J. Chem. Phys. E* **1973**, *6*, 1208–1210. (c) He, M.-Y.; Xiong, G.; Toscano, P. J.; Burwell, R. L., Jr.; Marks, T. J. *J. Am. Chem. Soc.* **1985**, *107*, 641–652.

(11) (a) Maecker, A. *Org. React.* **1965**, *14*, 270. (b) Maryanoff, B. E.; Reitz, A. B. *Chem. Rev.* **1989**, *89*, 863–927.

(12) (a) Ambuehl, J.; Pregosin, P. S.; Venanzi, L. M.; Consiglio, C.; Bachech, B.; Zambonelli, L. *J. Organomet. Chem.* **1979**, *181*, 255–269. (b) Ambuehl, J.; Pregosin, P. S.; Venanzi, L. M.; Ughetto, G.; Zambonelli, L. *J. Organomet. Chem.* **1978**, *160*, 329–335.

(13) Birtwistle, J. S.; Lee, K.; Morrison, J. D.; Sanderson, W. A.; Mosher, H. *J. Org. Chem.* **1964**, *29*, 37–40.

support. Gas chromatography/electron impact mass spectra were obtained using a Hewlett/Packard 5890 GC interfaced to a VG-70-250 SE spectrometer. A 15 M narrow bore J + W Scientific DB-1 fused silica capilliary with 1.0 μm film thickness was employed as the column material. An ion source potential of 70 eV, an inlet source temperature of 200 °C, and a column temperature ramp rate of 10 °C/min from ambient to 200 °C were used in GC/MS experiments. All mass spectra were calibrated using PCR perfluorokerosene 755.

Synthesis of (*S*)-(+)-2-Phenylbutyl Tosylate. A 100 mL three-neck flask equipped with a pressure-equalizing addition funnel and gas inlet adapter was charged under argon purge with degassed (*S*)-(+)-2-phenylbutanol (1.8 g, 12 mmol) and THF (30 mL). The colorless solution was cooled to −20 °C, *n*-BuLi (5 mL, 12.5 mmol of a 2.5 M solution in hexanes) was added via syringe, and the reaction mixture was stirred at −20 °C for 0.5 h. To this mixture was added dropwise a solution of *p*-toluenesulfonyl chloride (2.51 g, 13.2 mmol) in THF (10 mL). The resulting orange solution was stirred at −20 °C for 1 h, warmed to 25 °C, and quenched with water (20 mL). The organic solvent was removed on a rotary evaporator, and the water phase was extracted with diethyl ether (3 × 20 mL). The ether phase was dried over K_2CO_3–Na_2SO_4, filtered, and rotary evaporated at 25 °C to afford a slightly yellow oil. Crystallization from diethyl ether/pentane (1:5, v:v) yielded clear colorless needles of (*S*)-(+)-2-phenylbutyl tosylate (3.2 g, 88%).

^{1}H NMR ($CDCl_3$): δ 7.65 (d, *J* = 8.2 Hz, 2H), 7.25 (m, 5H), 7.06 (d, *J* = 7.2 Hz, 4H), 4.10 (m, 2H), 3.80 (m, 1H), 2.42 (s, 1H), 1.8 (m, 1H), 1.55 (m, 1H), 0.75 (t, *J* = 7.3 Hz, 3H). ^{13}C NMR ($CDCl_3$): δ 144.6, 140.3, 132.9, 129.8, 128.6, 127.9, 127.8, 127.0, 73.8, 46.8, 24.8, 21.7, 11.6. $[\alpha]_D^{25}$ = +14.4° (*c* = 1.0 in 95% EtOH, *l* = 0.5 dm).

Synthesis of (*S*)-(+)-2-Phenylbutane. A 100 mL three-neck flask equipped with a pressure-equalizing addition funnel and gas inlet adapter was charged with (*S*)-(+)-2-phenylbutyl tosylate (3.0 g, 9.9 mmol) and THF (30 mL). Under argon flush, $LiBHEt_3$ (30 mL, 30 mmol of a 1 M solution in THF, Aldrich) was quickly syringed into the mixture, and the resulting solution was stirred at 25 °C for 12 h. The reaction was quenched with water (50 mL), the organic solvent was removed under vacuum, and the aqueous phase was extracted with diethyl ether (3 × 30 mL). The ether phase was dried over K_2CO_3–Na_2SO_4, filtered, concentrated, and fractionally distilled under vacuum to yield 0.9 g (68%) of (*S*)-(+)-2-phenylbutane.

^{1}H NMR ($CDCl_3$): δ 7.30 (m, 2H), 7.13 (m, 3H), 2.53 (m, 1H), 1.55 (m, 2H), 1.22 (d, *J* = 7.6 Hz, 3H), 0.82 (t, 7.1 Hz, 3H). ^{13}C NMR ($CDCl_3$): δ 129.8, 127.3, 126.9, 125.7, 41.7, 31.6, 22.0, 12.6. $[\alpha]_D^{25}$ = +28.1° (*c* = 1.0 in 95% EtOH, *l* = 0.5 dm).

Preparative Scale Asymmetric Hydroamination/Cyclization. In the glovebox, a 20 mL cylindrical Pyrex reaction vessel, equipped with a Teflon inlet valve and a magnetic stirrer, was charged with Me_2SiCp''-(R*Cp)LnE($SiMe_3$)$_2$ (E = N, CH) (25–35 mg, ~0.05 mmol). On the vacuum line, pentane (2 mL) was condensed into the reaction apparatus *in vacuo* at −78 °C, followed by the amino olefin (0.60 mL, ~8.0 mmol). The mixture was warmed to ambient temperature (22 °C ± 1 °C). For the Ln = Nd and Sm catalysts, a characteristic color change from green and orange for the hydrocarbyl complexes to blue and yellow occurred, respectively. For the lanthanides having large ionic radii (La, Nd, Sm), the reactions were worked up after 1–12 h, while the reactions catalyzed by the lanthanides of smaller ionic radius (Y, Lu) were worked up after 1–3 days. Additionally, the Nd and Sm catalyst solutions turned from blue and yellow to green and orange, respectively, upon completion of catalytic turnover. The reaction mixtures were freeze–pump–thaw degassed at −78 °C, and the volatile components were subsequently vacuum-transferred twice into clean receiver flasks at −78 °C. Pentane was then removed at 0 °C on the rotary evaporator, affording a pale yellow liquid. ^{1}H NMR (C_6H_6) and GC/MS indicated clean, quantitative conversion to product heterocycle except for the least active catalysts, in which percent conversion was determined from the relative intensities of the olefinic (substrate) and exocyclic methyl (product) resonances. Enantiomeric excesses (ee values) were determined by measurement of optical rotation[14] and diastereomeric derivatization with (*R*)-(+)-α-methoxy-α-(trifluoromethyl)phenylacetyl chloride.[15] For the latter assay, ^{19}F NMR ($CDCl_3$) of the diastereomeric mixture of amides at 50 °C displayed two resonances, and the relative integration was used to determine percent ee.

Kinetic Study of Asymmetric Hydroamination/Cyclization. In a typical experiment, a 5 mm NMR tube with Teflon valve was charged with the organolanthanide precatalyst (5–10 mg) in the glovebox. On the vacuum line, toluene-d_8 (0.6–0.7 mL) was vacuum-transferred into the NMR tube at −78 °C. Sufficient amino olefin was subsequently introduced to establish an approximately 0.1 M solution (ca. 40–50 equiv of substrate/catalyst). The NMR tube was then back-filled with argon to ambient pressure and maintained at −78 °C until kinetic measurements were initiated. Meanwhile, the probe of the Varian XL-400 was equilibrated at the appropriate temperature (*T* ± 0.4 °C; checked with a methanol or ethylene glycol standard). The sample was then inserted and an initial (*t* = 0) spectrum recorded. A long pulse delay (10 s) was used during data acquisition to prevent saturation of the signal. The kinetics were monitored by the disappearance of the olefinic resonances of the substrate. The relative concentration of substrate (vs organolanthanide), *C*, was determined from the area of the ^{1}H-normalized integrals of the substrate olefinic resonances (A_s) standardized to the resonance of free $CH_2(SiMe_3)_2$ or $HN(SiMe_3)_2$ $SiMe_3$ groups (A_1). These species are released in the formation of the active catalyst via protonolytic cleavage of the corresponding precursor by the amine substrate. Kinetic data for the hydroamination reaction were fit by least-squares methods to eq 2, where

$$(C_0 - C) = mt \qquad (2)$$

$C_0(A_{s0}/A_{10})$ is the initial concentration of substrate (relative to organolanthanide) and $C(A_s/A_1)$ is the substrate concentration at time, *t*. The turnover frequency (N_t, h^{-1}) was calculated from the least-squares determined slope (*m*) of the resulting plot.

Preparative Scale Asymmetric Hydrogenation. All preparative scale hydrogenation experiments were performed on a vacuum line with a mercury manometer arrangement as previously described.[16] In a typical experiment, a 50 mL cylindrical Pyrex reaction vessel, equipped with a magnetic stirrer, was charged in the glovebox with Me_2SiCp''(R*Cp)-LnCH($SiMe_3$)$_2$ (20–30 mg, 0.04–0.05 mmol), 2-phenyl-1-butene or styrene (0.98 mL, ~6.5 mmol), and freshly vacuum-transferred heptane (4 mL). On the vacuum line, the mixture was freeze–pump–thaw degassed twice at −78 °C. The reaction vessel was then placed in a thermostated bath (±1 °C). Hydrogen (760 Torr) was introduced, and rapid stirring was initiated. Hydrogen uptake was immediately evident from the rise in the mercury column. In addition, a rapid color change of the reaction solution from the color of the parent hydrocarbyl complex to a deep red occurred immediately after H_2 introduction. After 30–60 min, hydrogen uptake ceased. A concomitant color change from deep red to the color of the parent organolanthanide hydride occurred. The mixture was freeze–pump–thaw degassed twice; the volatile components were then vacuum-transferred twice into clean receiver flasks at −78 °C. GLC sampling of the volatile mixture indicated the presence of only *n*-heptane and 2-phenylbutane in significant amounts. These compounds were identified by co-injection with authentic samples. Heptane was subsequently removed via rotary evaporation. Yield: 0.85 g (95%) of 2-phenylbutane.

The ^{1}H NMR of this sample indicated clean conversion with only a trace of $CH_2(SiMe_3)_2$ from hydrogenolysis of the precursor hydrocarbyl functionality. Enantiomeric excesses were determined from the optical rotation (*c* = ~1.0 in 95% ethanol, 26 °C).[17]

Kinetics of Catalytic Enantioselective Hydrogenation. Kinetic studies were performed the all-glass, metal, and Teflon grease-free, constant-volume, pseudo-constant-pressure, gas-uptake apparatus described previously.[6a] In a typical experiment, the oven-dried, jacketed reactor was attached to the vacuum line while still hot, evacuated/back-filled with argon 5–7 times, and finally evacuated continuously for at least 1 h (ultimate vacuum attainable, 2–4 × 10^{-6} Torr). The burets were back-filled with argon and sealed, and the entire reaction vessel was transported into the glovebox. The burets were then filled with freshly-prepared volumetric solutions of Me_2SiCp''(R*Cp)SmCH($SiMe_3$)$_2$ and 2-phenyl-1-butene in *n*-heptane. The burets were tightly sealed, and the entire apparatus was quickly transported outside to the vacuum line. The reaction volume was evacuated/back-filled with argon (more efficient displacement of air and moisture) until the ultimate vacuum achievable

(14) (a) Ringdahl, B.; Pereira, W. E., Jr.; Craig, J. C. *Tetrahedron* **1981**, *37*, 1659–1662. (b) Absolute configuration assigned from the $[\alpha]_D$ value for the analogous pyrrolidines.[14a,c,d] (c) Craig, J. C.; Roy, S. K. *Tetrahedron* **1965**, *21*, 401–406. (d) Ripperger, H.; Schreiber, K. *Tetrahedron* **1965**, *21*, 407–412.

(15) Dale, J. A.; Dull, D. L.; Mosher, H. S. *J. Org. Chem.* **1969**, *34*, 2543–2549.

(16) (a) Fagan, P. J.; Manriquez, J. M.; Maatta, E. A.; Seyam, A. M.; Marks, T. J. *J. Am. Chem. Soc.* **1981**, *103*, 6650–6667. (b) Fagan, P. J. Ph.D. Thesis, Northwestern University, Evanston, IL, 1980.

(17) Lardicci, L.; Menicagli, R.; Salvadori, P. *Gazz. Chim. Ital.* **1968**, *98*, 738–759.

was <2 × 10^{-6} Torr. The apparatus was subsequently evacuated/backfilled with hydrogen repetitively—usually 5–6 times—to ensure complete removal of argon. On the ultimate evacuation cycle, the pressure was recorded from a mercury manometer. The entire system was then filled with hydrogen and adjusted to the desired pressure. A thermostated (±0.2 °C) water circulating system was connected to the reactor water jacket and actuated. After all components had attained thermal equilibrium and equilibrium with the reactor atmosphere, a measured volume of olefin solution (0.45–0.50 mL) was titrated into the reactor. For preparative scale reactions under non-mass-transport-limited conditions, 1.0–1.5 mL of neat olefin was used at 750 Torr. Vortex mixing was briefly initiated to equilibrate the atmosphere with solvent vapor and to grossly adjust the mixing speed. Agitation was then terminated, and the mixture was allowed to settle completely. A final pressure reading was recorded from the manometer. Next, the catalyst solution was quickly measured into the reaction vessel (ca. 0.45–0.50 mL). High-speed vortex mixing was initiated, and the change in hydrogen pressure was recorded as a function of time using the previously described electronic manometer.[6a] Appropriate corrections were made for solvent vapor pressure. In general, conditions were adjusted such that consumption of olefin was complete within 1–10 min and the overall pressure drop was always less than 2% (usually <1%). Since, under all conditions of substrate and catalyst concentration and total reaction volume employed, turnover frequencies (N_t) were approximately 1 order of magnitude lower than those previously observed under identical conditions (e.g., for the $(Cp_2'LuH)_2$-catalyzed hydrogenation of 1-hexane),[6a] mass transport effects were judged to be negligible. Reproducibility in N_t values for the same reaction at the same H_2 pressure and catalyst concentration using different batches of olefin and catalyst solution was within 5–10%. The data were fit via least-squares analysis to eq 3, where C_0 is the initial olefin concentration

$$(C_0 - C) = mt \tag{3}$$

and C is the concentration at time, t. Since the reactions were performed under pseudo-zeroth-order conditions of hydrogen pressure and no catalyst decomposition was detectable (for $[Ln]_T > 0.4$ mM), the turnover frequency (N_t, h^{-1}) was determined for a given catalyst concentration and hydrogen pressure by eq 4, where m is the reaction rate from eq 3 and $[Ln]_T$ is the total concentration of catalyst precursor.

$$N_t\,(h^{-1}) = m/[Ln]_T \tag{4}$$

Results

The goal of this investigation was to examine the scope, stereoselectivity, Ln sensitivity, and mechanism of two well-defined, organolanthanide-catalyzed olefin transformations mediated by the present chiral C_1-symmetric hydrocarbyl and amide complexes. The stereoselective hydroamination/cyclization of amino olefins is discussed first, followed by the asymmetric hydrogenation of α-ethylstyrene and the deuteration of styrene. The discussions include mechanistic implications of the kinetic and stereoselectivity studies as well as the possible molecular basis for enantioselection. The present hydrocarbyl and amide precatalysts provide the first insights into asymmetric organolanthanide catalysis. Structure/reactivity patterns emerge, and several aspects of the catalyst configuration and configurational stability will be seen to play a major role.

Asymmetric Organolanthanide-Catalyzed Hydroamination/Cyclization. The complexes Cp'_2LnR and $Me_2SiCp''_2LnR$ (R = $E(SiMe_3)_2$ (E = CH, N), η^3-allyl, and H) efficiently and regiospecifically catalyze the intramolecular hydroamination/cyclization of N-unprotected amino olefins to the corresponding 2-methylheterocycles.[9] This cyclization process, illustrated in eq 5 for the conversion of aminopent-4-enes to 2-methylpyrrolidines and 2,2-dimethyl-1-aminohex-5-ene to 2,5,5-trimethylpiperidine, generates a new asymmetric center adjacent to the heterocyclic nitrogen atom. The products are racemic with $Cp'_2LnE(TMS)_2$ and $Me_2SiCp''_2LnE(TMS)_2$ (E = CH, N) as precatalysts.[9] However, the chiral complexes $Me_2SiCp''(R^*Cp)LnE(TMS)_2$ (E = CH, N) efficiently catalyze this process under identical conditions with high enantioselectivity. Kinetic and

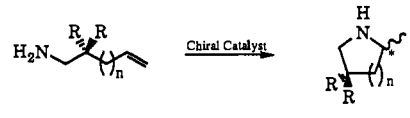

(5)

8, R = H, n=1
9, R = CH_3, n = 1
10, R = CH_3, n = 2

11, R = H, n=1
12, R = CH_3, n = 1
13, R = CH_3, n = 2

enantioselection data for the hydroamination/cyclization of several achiral amino olefins are presented in Table 1.

Under identical conditions, the present initial turnover frequencies are ~10 times those of the Cp'_2Ln-catalyzed reactions,[9] likely reflecting enhanced coordinative unsaturation at the metal center. However, for constant substrate, the dependence of N_t on Ln^{3+} ionic radius scales in approximately the same order for the chiral and achiral catalysts, while the dependence of N_t on substrate for constant catalyst (**9** > **8** > **10**) is also similar. Furthermore, N_t values are indistinguishable for chiral precatalysts having E either CH or N. This latter observation is compatible with *in situ* ^1H NMR studies which reveal rapid protonolytic displacement of the corresponding $HE(TMS)_2$ fragment as turnover commences. The enantioselectivities observed for the present catalytic hydroamination/cyclizations are relatively high, 69% and 64% ee for (*S*)-(+)-2-methylpyrrolidine with (*R*)-**6g**/**7f** and (*R*)-**6i** (entries 14 and 15), respectively, at 25 °C. Also, enantioselectivities increase as the temperature is decreased, from 53% ee at 25 °C to 74% ee at −30 °C for the cyclization **9** → **12** with (*S*)-**7e** (entries 26–28). The configurations and optical purities of the product heterocycles depend on chiral ancillary ligand, Ln, and temperature but interestingly are *insensitive to the optical purity of the precatalyst*. Thus, within experimental error, both epimers of all precatalysts examined yield heterocyclic products in preparative scale reactions of the same sign and approximately the same ee (cf. Table 1 entries 1 + 2, 5 + 6, 9 + 11, 12 + 13, 22 + 23, 24 + 25, and 31 + 32). It will be seen that this behavior reflects the tendency of these complexes to undergo epimerization[1] in the presence of N–H bearing amines (*vide infra*).

The (+)-neomenthyl and (−)-menthyl/(−)-phenylmenthyl catalyst classes preferentially mediate the formation of *opposite* optical antipodes for both 2-methylpyrrolidine (**11**) and 2,4,4-trimethylpyrrolidine (**12**) (Table 1). The relative stereodifferentiating efficiencies of the (+)-neomenthyl, (−)-menthyl, and (−)-phenylmenthyl auxiliaries range from small to moderate for constant metal and substrate (cf. entries 6/7 + 9/11, 13 + 14 + 15, 19 + 26, 22 + 29 + 31, and 33 + 34). There is also a marked sensitivity of asymmetric induction to the identity/size of the Ln ion. For the (+)-neomenthyl series of catalysts, an increase in catalytic enantioselectivity occurs on traversing the lanthanide series from La^{3+} (**6/7a**) through the (smaller) Sm^{3+} complex (**6c/7b**), with the enantioselectivity decreasing thereafter and ultimately favoring the opposite (*S*) product antipode for Lu^{3+} (Figure 1). A similar trend is observed for the (−)-menthyl catalysts in which the enantioselection increases from Ln = Sm to Ln = Y and then likewise decreases, with Ln = Lu giving the opposite (*R*) product enantiomer. In regard to substrate, Table 1 indicates similar stereodifferentiating efficiencies for aminopentenes **8** and **9** but an erosion in the case of aminohexene **10**. Control experiments reveal, importantly, that achiral catalysts do not epimerize optically-enriched samples of product heterocycles and that chiral catalysts do not impart any optical enrichment to racemic products under catalytic conditions. Both of these observations support operationally irreversible olefin insertion/cyclization.

In principle, diastereoselective processes should also be mediated by the species derived from the chiral $Me_2SiCp''(R^*Cp)LnE(TMS)_2$ (E = CH, N) precatalysts. Indeed, **6b** and **6c/7b** effect the clean, rapid cyclization of 2-aminohex-5-ene at 25 °C

Table 1. Rate, Product Enantiomeric Excess, and Absolute Configuration Data for Catalytic Hydroamination/Cyclization of Aminopent-4-ene (**8**), 2,2-Dimethyl-1-aminopent-4-ene (**9**), and 2,2-Dimethyl-1-aminohex-5-ene (**10**) Mediated by Various Chiral Organolanthanide Catalysts[a]

entry	substrate	precatalyst[b]	precatalyst structure	t (°C)	N_t (h^{-1})	enantiomeric excess (%) (sign)
1	**8**	(*R,S*)-**6a**	(*R,S*)-neomenthylLaCH(TMS)$_2$	25		36 (−)[c]
2	**8**	(*R*)-**7a**	(*R*)-neomenthylLaN(TMS)$_2$	25		31 (−)[c]
3	**8**	(*R,S*)-**6b**	(*R,S*)-neomenthylNdCH(TMS)$_2$	25	93	55 (−)[c]
4	**8**	(*R,S*)-**6b**	(*R,S*)-neomenthylNdCH(TMS)$_2$	0	11	64 (−)[c]
5	**8**	(*R,S*)-**6c**	(*R,S*)-neomenthylSmCH(TMS)$_2$	25	42	61 (−)[c]
6	**8**	(*S*)-**7b**	(*S*)-neomenthylSmN(TMS)$_2$	25	33	55 (−)[c]
7	**8**	(*R*)-**6c**/**7b**	(*R*)-neomenthylSmCH(TMS)$_2$/N(TMS)$_2$	25	62	52 (−)[c]
8	**8**	(*R*)-**6c**/**7b**	(*R*)-neomenthylSmCH(TMS)$_2$/N(TMS)$_2$	0		58 (−)[c]
9	**8**	(*S*)-**7e**	(*S*)-menthylSmN(TMS)$_2$	25	33	62 (+)[c]
10	**8**	(*S*)-**7e**	(*S*)-menthylSmN(TMS)$_2$	0		72 (+)[c]
11	**8**	(*R*)-**7e**	(*R*)-menthylSmN(TMS)$_2$	25		60 (+)[c]
12	**8**	(*R,S*)-**6d**	(*R,S*)-neomenthylYCH(TMS)$_2$	25	4	47 (−)[c]
13	**8**	(*R*)-**7c**	(*R*)-neomenthylYN(TMS)$_2$	25		50 (−)[c]
14	**8**	(*R*)-**6g**/**7f**	(*R*)-menthylYCH(TMS)$_2$/N(TMS)$_2$	25		69 (+)[c]
15	**8**	(*R*)-**6l**	(*R*)-phenylmenthylYCH(TMS)$_2$	25		64 (+)[c]
16	**8**	(*R,S*)-**6e**	(*R,S*)-neomenthylLuCH(TMS)$_2$	25		29 (+)[c]
17	**9**	(*R*)-**7a**	(*R*)-neomenthylLaN(TMS)$_2$	25		14 (−)[d]
18	**9**	(*R,S*)-**6b**	(*R,S*)-neomenthylNdCH(TMS)$_2$	−20		61 (−)[d]
19	**9**	(*R*)-**6c**/**7b**	(*R*)-neomenthylSmCH(TMS)$_2$/N(TMS)$_2$	25		51 (−)[d]
20	**9**	(*R*)-**6c**/**7b**	(*R*)-neomenthylSmCH(TMS)$_2$/N(TMS)$_2$	0		54 (−)[d]
21	**9**	(*R*)-**6c**/**7b**	(*R*)-neomenthylSmCH(TMS)$_2$/N(TMS)$_2$	−30		64 (−)[d]
22	**9**	(*R,S*)-**6d**	(*R,S*)-neomenthylYCH(TMS)$_2$	25	38	36 (−)[d]
23	**9**	(*R*)-**7c**	(*R*)-neomenthylYN(TMS)$_2$	25	21	40 (−)[d]
24	**9**	(*R,S*)-**6e**	(*R,S*)-neomenthylLuCH(TMS)$_2$	25		36 (+)[d]
25	**9**	(*R*)-**7d**	(*R*)-neomenthylLuN(TMS)$_2$	25		40 (+)[d]
26	**9**	(*S*)-**7e**	(*S*)-menthylSmN(TMS)$_2$	25	84	53 (+)[d]
27	**9**	(*S*)-**7e**	(*S*)-metnyhlSmN(TMS)$_2$	0		61 (+)[d]
28	**9**	(*S*)-**7e**	(*S*)-menthylSmN(TMS)$_2$	−30		74 (+)[d]
29	**9**	(*R*)-**6g**/**7f**	(*R*)-menthylYCH(TMS)$_2$/N(TMS)$_2$	25	9	43 (+)[d]
30	**9**	(*R*)-**6h**	(*R*)-menthylLuCH(TMS)$_2$	25		29 (−)[d]
31	**9**	(*R*)-**6l**	(*R*)-phenylmenthylYCH(TMS)$_2$	25	8	56 (+)[d]
32	**9**	(60/40) (*R/S*)-**7h**	(*R,S*)-phenylmenthylYN(TMS)$_2$	25		54 (+)[d]
33	**10**	(*S*)-**7e**	(*S*)-menthylSmN(TMS)$_2$	25	2	15 (−)[d]
34	**10**	(*R*)-**6c**/**7b**	(*R*)-neomenthylSmCH(TMS)$_2$/N(TMS)$_2$	25		17 (−)[d]

[a] Conditions: [substrate]/[catalyst], (40–200)/1; solvent, pentane; 100% conversion and >95% regiospecificity by GLC and ^{1}H NMR measurements. N_t calculated from first half-life. [b] See Scheme 1 for a key to precatalyst numbering. [c] References 14a and 15. $[\alpha]^{20}_D$ = −20.0° for (*R*)-(−)-2-methylpyrrolidine. [d] References 14b and 15. $[\alpha]^{20}_D$ = −24.3° for (*R*)-(−)-2,4,4-trimethylpyrrolidine.

(substrate:catalyst > 100:1) to yield the C_2-symmetric auxiliary[18] *trans*-2,5-dimethylpyrrolidine[18] with >95% diastereoselectivity (eq 6). Under identical conditions, achiral Cp′$_2$Ln/Me$_2$SiCp″Ln

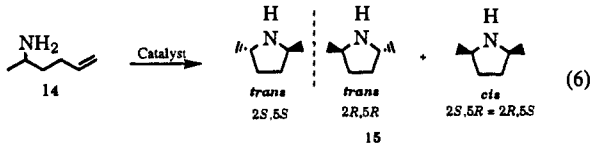

(6)

(Ln = Nd, Sm) precatalysts afford only modest diastereoselection (1:1–3:1, *trans*:*cis*).[9c] Since the substrate of eq 6 is racemic, the product is racemic at 100% conversion, as anticipated. However, (*S*)-**14** and (*R*)-**14** should undergo cyclization at different rates at a chiral catalyst, and at <100% conversion it should be possible, in principle, to isolate, via kinetic resolution,[19] optically active *trans*-**15**. Survey experiments in which the reaction was quenched at various extents of conversion indicate that product enrichments achievable are modest (<20% ee at 25 °C).

The kinetics of enantioselective hydroamination/cyclization were investigated by *in situ* ^{1}H NMR. The disappearance of the olefinic ^{1}H substrate resonances was monitored as a function of time in the presence of the Me$_2$SiCp″(R*Cp)LnR catalyst precursors. In general, a 40–50-fold molar excess of the substrate was employed in kinetic studies. The LnE(TMS)$_2$ bond undergoes rapid and irreversible protonolysis with generation of HE(TMS)$_2$, which in turn serves as a convenient internal NMR standard in a relatively signal-free spectral region. Turnover frequencies for the various cyclizations were determined from the slopes of the kinetic plots of substrate/catalyst ratio vs time; representative data are shown in Figure 2. The initial linear dependence of olefin concentration on time suggests essentially zeroth-order dependence of the catalytic rate on substrate concentration in analogy to achiral Cp′$_2$LnCH(SiMe$_3$)$_2$, Me$_2$SiCp″$_2$LnCH(SiMe$_3$)$_2$, and R$_2$SiCp″CpLnCH(SiMe$_3$)$_2$, arguing for a similar turnover-limiting intramolecular olefin insertion step.[9c] However, deviation from linearity is observed at high conversions for some catalyst–substrate combinations (Figure 2B). This apparently reflects competitive inhibition by the product heterocycle (*vide infra*). As noted above, hydroamination/cyclization rates decrease with decreasing Ln ionic radius and decreasing temperature (Table 1) as for the achiral catalysts.[9] However, in marked contrast to the more saturated catalysts, *in situ* ^{1}H NMR experiments with the present paramagnetic Nd^{3+} (**4f**^{3}) and Sm^{3+} (**4f**^{5}) catalysts reveal that product resonances are *paramagnetically broadened* after ~1 half-life, which implies that the product heterocycles are involved in coordination to/amine exchange with the chiral paramagnetic lanthanide amine–amido complexes (Cp′$_2$LnNHR(NH$_2$R)$_x$, *vide infra*).[9c] The product heterocycles thus appear capable of functioning as competitive inhibitors—a role similar to that observed for *n*-propylamine in the achiral catalytic systems.[9c]

In situ ^{1}H NMR experiments also indicate that the chiral hydrocarbyl and amide complexes rapidly and quantitatively form, by analogy to the achiral systems,[9c] amine–amido adducts in the

(18) (a) Harding, K. E.; Burks, S. R. *J. Org. Chem.* **1981**, *46*, 3920–3922. (b) Whitesell, J. K.; Felman, S. W. *J. Org. Chem.* **1977**, *42*, 1663–1664.

(19) For reviews and applications of kinetic resolution, see: (a) Finn, M. G.; Sharpless, K. B. In *Asymmetric Synthesis*; Morrison, J. D., Ed.; Academic: New York, 1985; Chapter 8. (b) Kagan, H. B.; Fiaud, J. C. *Top. Stereochem.* **1988**, *18*, 249–330. (c) Chen, C.-S.; Sih, C. J. *Angew. Chem., Int. Ed. Engl.* **1989**, *28*, 695–707. (d) Martin, V. S.; Woodward, S. S.; Katsuki, T.; Yamada, Y.; Ikeda, M.; Sharpless, K. B. *J. Am. Chem. Soc.* **1981**, *103*, 6237–6240. (e) Woodward, S. S.; Finn, M. G.; Sharpless, K. B. *J. Am. Chem. Soc.* **1991**, *113*, 106–113. (f) VanNieuwenhze, M. S.; Sharpless, K. B. *J. Am. Chem. Soc.* **1993**, *115*, 7864–7865.

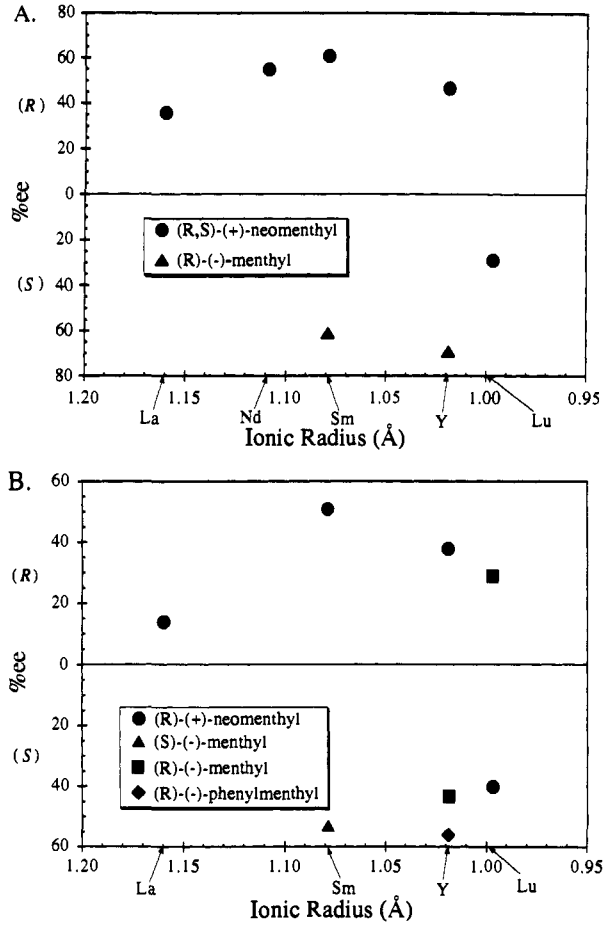

Figure 1. Plot of ee as a function of eight-coordinate Ln^{3+} ionic radius and chiral auxillary (R*). (A) Hydroamination/cyclization of 1-aminopent-4-ene (**8**) to 2-methylpyrrolidine (**11**). (B) Hydroamination/cyclization of 2,2-dimethyl-1-aminopent-5-ene (**9**) to 2,4,4-trimethylpyrrolidine (**12**) mediated by the indicated $Me_2SiCp''(R^*)LnE(SiMe_3)_2$ precatalysts.

presence of *n*-propylamine (eq 7). These adducts are in rapid

$$Me_2SiCp''(R^*Cp)LnR + 2H_2NR' \rightarrow Me_2SiCp''(R^*Cp)Ln(NHR')(NH_2R') + RH \quad (7)$$

exchange on the NMR time scale with free *n*-propylamine. The amine–amido complexes also undergo epimerization under catalytic reaction conditions (e.g., eq 8) to afford mixtures of (*R*)- and (*S*)-configurational isomers.[1] For the homochiral (+)-

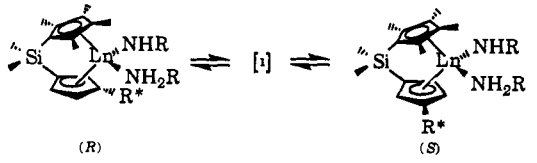

(8)

neomenthyl precatalysts, an 80:20 (*R*):(*S*) epimer ratio is established in the presence of a 40–50-fold excess of *n*-propylamine within ~2 h at 25 °C. Under the same conditions and on approximately the same time scale, the (–)-menthyl and (–)-phenylmenthyl complexes lead to >95:5 and ~90:10 (*S*):(*R*) equilibrium ratios, respectively. The kinetic data for the epimerization of **6i**/**7h** and **6f**/**7e** in excess *n*-propylamine[1] indicate that this rearrangement is competitive with the rate of the hydroamination and is more facile for the larger lanthanide ions. This epimerization process plausibly explains the virtual independence of the optical purity of the product on the initial optical purity and configuration of the precatalyst (Table 1, *vide infra*). In preparative scale catalytic reactions, greater than 200 equiv of

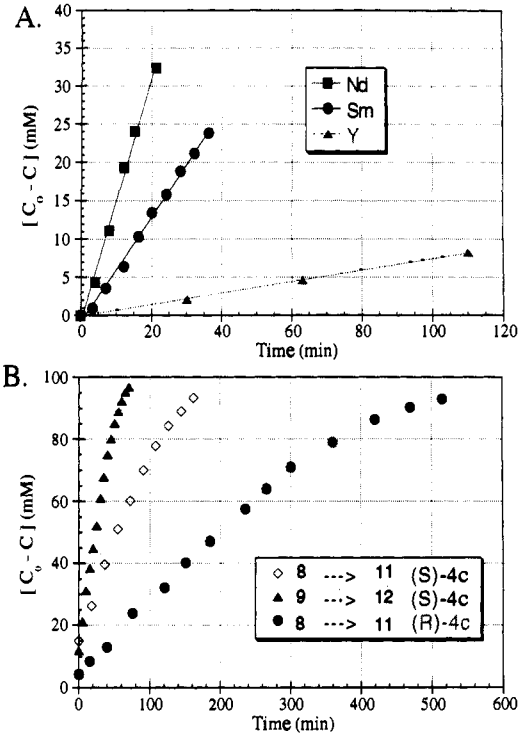

Figure 2. (A) Plot of normalized [substrate(A_0) – substrate(A_t)] as a function of time for the hydroamination/cyclization of $H_2N(CH_2)_3CH{=}CH_2$ (**8**) using precatalysts (*R*,*S*)-Me_2SiCp''[(+)-neomenthylCp]-$LnCH(TMS)_2$ (Ln = Nd [(*R*,*S*)-**6b**], Sm [(*R*,*S*)-**6c**], Y [(*R*,*S*)-**6d**] in toluene-d_8. The line is the least-squares fit to the data points. (B) Plot of normalized [substrate(A_0)–substrate(A_t)] as a function of time for the hydroamination/cyclization of $H_2N(CH_2)_3CH{=}CH_2$ (**8**) and $H_2NCH_2C(CH_3)_2CH_2CH{=}CH_2$ (**9**) using precatalysts (*R*)- and (*S*)-Me_2SiCp''[(–)menthylCp]$SmN(TMS)_2$ [(*R*)- and (*S*)-**7e**] in toluene-d_8.

substrate (~0.5 mol % catalyst) are typically used. Such substrate/catalyst ratios should accelerate epimerization, assuming an associative epimerization mechanism, and should ensure complete epimerization at low substrate conversions.[1] Efforts to accurately measure catalyst epimerization ratios in the presence of normal substrate amounts in preparative scale reactions were frustrated by the complexity of the NMR spectra.

Catalytic Enantioselective Hydrogenation. The efficacy of the present chiral complexes as precatalysts for asymmetric hydrogenation and deuteration was assayed with the styrenic olefins 2-phenyl-1-butene and styrene (eq 9). These unfunctionalized

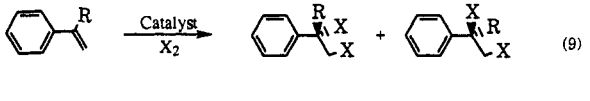

(9)

olefins are typically difficult substrates to reduce with substantial enantioselectivity and at appreciable rates.[20-22] Moreover, the

(20) (a) Moriarty, K. J.; Rogers, R. D.; Paquette, L. A. *Organometallics* **1989**, *8*, 1512–1517. (b) Paquette, L. A.; Moriarty, K. J.; Rogers, R. D. *Organometallics* **1989**, *8*, 1506–1511. (c) Paquette, L. A.; Moriarty, K. J.; McKinney, J. A.; Rogers, R. D. *Organometallics* **1989**, *8*, 1707–1713. (d) Halterman, R. L.; Vollhardt, K. P. C. *Organometallics* **1988**, *7*, 883–892. (e) Halterman, R. L.; Vollhardt, K. P. C.; Welker, M. E.; Bläser, D.; Boese, R. *J. Am. Chem. Soc.* **1987**, *109*, 8105–8107. (f) Paquette, L. A.; McKinney, J. A.; McLaughlin, M. L.; Rheingold, A. L. *Tetrahedron Lett.* **1986**, *27*, 5599–5602. (g) Halterman, R. L.; Vollhardt, K. P. C. *Tetrahedron Lett.* **1986**, *27*, 1461–1464. (h) Couturier, S.; Tainturier, G.; Gautheron, B. *J. Organomet. Chem.* **1980**, *195*, 291–306. (i) Dormond, A.; El Bouadili, A.; Moise, C. *Tetrahedron. Lett.* **1983**, *24*, 3087–3089. (j) Le Blanc, J. C.; Moise, C.; Tirouflet, J. *J. Organomet. Chem.* **1978**, *148*, 171–178. (k) Cesarotti, E.; Kagan, H. B.; Goddard, R.; Kruger, C. *J. Organomet. Chem.* **1978**, *162*, 297–309. (l) Le Blanc, J. C.; Moise, C. *J. Organomet. Chem.* **1976**, *120*, 65–71.

Table 2. Product Enantiomeric Excess and Absolute Configuration Data for Hydrogenation of 2-Phenyl-1-butene and Deuteration of Styrene by Chiral Organolanthanide Catalysts[a]

entry	substrate	precatalyst[b]	precatalyst structure	t (°C)	enantiomeric excess (%) (sign)	k_{H_2}/k_{D_2}
1	α-ethylstyrene	(*R*,*S*)-**6a**	(*R*,*S*)-neomenthylLaCH(TMS)$_2$	25	58 (–)	
2	α-ethylstyrene	(*R*,*S*)-**6b**	(*R*,*S*)-neomenthylNdCH(TMS)$_2$	25	40 (–)	
3	α-ethylstyrene	(*R*,*S*)-**6c**	(*R*,*S*)-neomenthylSmCH(TMS)$_2$	25	19 (–)	
4	α-ethylstyrene	(*R*,*S*)-**6c**	(*R*,*S*)-neomenthylSmCH(TMS)$_2$	25	46 (–)[c]	
5	α-ethylstyrene	(*R*,*S*)-**6c**	(*R*,*S*)-neomenthylSmCH(TMS)$_2$	–20	42 (–)	
6	α-ethylstyrene	(*R*,*S*)-**6c**	(*R*,*S*)-neomenthylSmCH(TMS)$_2$	–35	51 (–)	
7	α-ethylstyrene	(*R*,*S*)-**6c**	(*R*,*S*)-neomenthylSmCH(TMS)$_2$	–78	60 (–)	
8	α-ethylstyrene	(*R*)-**6c**	(*R*)-neomenthylSmCH(TMS)$_2$	25	71 (–)	
9	α-ethylstyrene	(*R*)-**6c**	(*R*)-neomenthylSmCH(TMS)$_2$	25	73 (–)[c]	2.1
10	α-ethylstyrene	(*R*)-**6c**	(*R*)-neomenthylSmCH(TMS)$_2$	0	61 (–)	
11	α-ethylstyrene	(*R*)-**6c**	(*R*)-neomenthylSmCH(TMS)$_2$	0	67 (–)[c]	
12	α-ethylstyrene	(*R*)-**6c**	(*R*)-neomenthylSmCH(TMS)$_2$	–78	71 (–)	
13	α-ethylstyrene	(*S*)-**6c**	(*S*)-neomenthylSmCH(TMS)$_2$	25	19 (+)[c]	1.5
14	α-ethylstyrene	(*S*)-**6c**	(*S*)-neomenthylSmCH(TMS)$_2$	0	17 (+)	
15	α-ethylstyrene	(*S*)-**6c**	(*S*)-neomenthylSmCH(TMS)$_2$	0	19 (+)[c]	
16	α-ethylstyrene	(*S*)-**6c**	(*S*)-neomenthylSmCH(TMS)$_2$	–78	14 (+)	
17	α-ethylstyrene	(*R*,*S*)-**6d**	(*R*,*S*)-neomenthylYCH(TMS)$_2$	25	12 (–)	
18	α-ethylstyrene	(*R*,*S*)-**6e**	(*R*,*S*)-neomenthylLuCH(TMS)$_2$	25	10 (–)	
19	α-ethylstyrene	(*R*)-**6f**	(*R*)-menthylSmCH(TMS)$_2$	25	8 (–)	
20	α-ethylstyrene	(*R*)-**6f**	(*R*)-menthylSmCH(TMS)$_2$	25	16 (–)[c]	2.3
21	α-ethylstyrene	(*R*)-**6f**	(*R*)-menthylSmCH(TMS)$_2$	0	16 (–)	
22	α-ethylstyrene	(*R*)-**6f**	(*R*)-menthylSmCH(TMS)$_2$	–20	22 (–)	
23	α-ethylstyrene	(*R*)-**6f**	(*R*)-menthylSmCH(TMS)$_2$	–30	27 (–)	
24	α-ethylstyrene	70/30 (*S*/*R*)-**6f**	(*S*/*R*)-menthylSmCH(TMS)$_2$	25	64 (+)	
25	α-ethylstyrene	70/30 (*S*/*R*)-**6f**	(*S*/*R*)-menthylSmCH(TMS)$_2$	25	80 (+)[c]	2.1
26	α-ethylstyrene	70/30 (*S*/*R*)-**6f**	(*S*/*R*)-menthylSmCH(TMS)$_2$	0	71 (+)	
27	α-ethylstyrene	70/30 (*S*/*R*)-**6f**	(*S*/*R*)-menthylSmCH(TMS)$_2$	–30	79 (+)	
28	α-ethylstyrene	70/30 (*S*/*R*)-**6f**	(*S*/*R*)-menthylSmCH(TMS)$_2$	–80	96 (+)	
29	α-ethylstyrene	(*R*)-**6g**	(*R*)-menthylYCH(TMS)$_2$	25	3 (–)	
30	styrene	(*R*)-**6f**	(*R*)-menthylSmCH(TMS)$_2$	25	43 (–)[c,d]	
31	styrene	70/30 (*S*/*R*)-**6f**	(*R*/*S*)-menthylSmCH(TMS)$_2$	25	72 (+)[c,d]	

[a] Conditions: [substrate]/[catalyst], (100–1000)/1; solvent, heptane; P_{H_2}, 760 Torr; rapid stirring; 100% conversion by GLC and ^{1}H NMR. [b] See Scheme 1 for key to precatalyst numbering. [c] Vortex mixing.[6a] [d] Based on $[\alpha]^{20}_D$ = +0.80° for (*S*)-(+)-phenylethane-1,2-d_2 (neat, l = 0.5 dm);[25] regiospecificity confirmed by ^{13}C NMR.

optical rotations of the product are significant (unlike the case of saturated hydrocarbons) and appear to be reliable and/or can be readily confirmed (see Experimental Section). In a typical procedure, a 200:1 molar ratio of substrate/catalyst was employed in heptane solution with P_{H_2} = 1 atm. The conversion of substrate to product is rapid, clean, and quantitative under these conditions. GLC and NMR of the crude product mixture indicate the presence of only 2-phenylbutane (or ethylbenzene), heptane, and trace amounts of $CH_2(SiMe_3)_2$. Deuteration studies substituting D_2 for H_2 give 2-phenylbutane-1,2-d_2 and ethylbenzene-1,2-d_2 exclusively as assayed by ^{13}C NMR and GC/MS. Presumably, the catalytically-active species is a Ln hydride generated via hydrogenolysis (eq 10) of the hydrocarbyl precatalysts.[1,4] The

$$2Me_2SiCp''(R^*Cp)LnCH(SiMe_3)_2 + 2H_2 \rightarrow [Me_2SiCp''(R^*Cp)LnH]_2 + 2CH_2(SiMe_3)_2 \quad (10)$$

organometallic products remaining after substrate consumption and vacuum-transfer of the volatile components exhibit ^{1}H NMR spectra identical to those of the independently-synthesized organolanthanide hydride complexes.[1] However, neither the isolated hydride complexes nor the residual catalyst solutions display the high activities exhibited by the *in situ* generated catalysts. This anomaly is not observed for the $(Cp'_2LnH)_2$ or $(Me_2SiCp''_2LnH)_2$ systems, which exhibit identical olefin hydrogenation activity, independent of the method of catalyst generation.[6] The present results imply that once formed, the presumed dimeric[1] hydrido complexes do not readily undergo dissociation. This may be due to ligand redistribution similar to that observed in the related achiral $Me_2SiCp''CpLn$ (Ln = Y, Lu) complexes (**A**, *vide supra*) or due to a small equilibrium constant for a $(\mu\text{-H})_n$ dissociation to reactive monomer (*vide infra*).

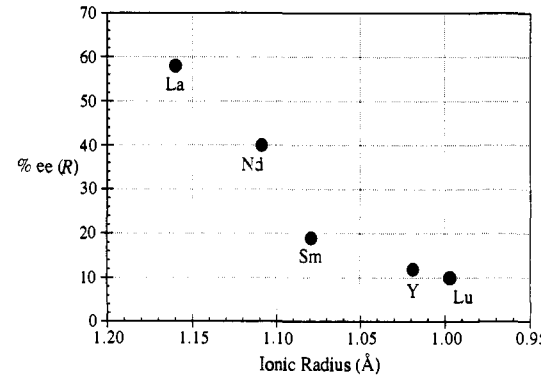

Figure 3. Plot of ee vs eight-coordinate lanthanide ionic radius for the hydrogenation of 2-phenyl-1-butene catalyzed by the precatalyst series (*R*,*S*)-Me_2SiCp'[(+)-neomenthylCp]LnCH(TMS)$_2$ at 25 °C.

The enantioselectivities for the hydrogenation of 2-phenyl-1-butene and deuteration of styrene display several noteworthy trends (Table 2). First, ee values are relatively high—the highest yet reported for the ambient temperature hydrogenation of these problematic (devoid of polar functional groups) substrates.[20–23] Enantioselection is very sensitive to the identity/size of Ln. For the isoleptic (*R*,*S*)-Me_2SiCp''[(+)-neomenthylCp]LnCH(TMS)$_2$ complexes, the ee decreases markedly with decreasing Ln ionic radius (Figure 3), and a similar trend obtains for the (*R*)-Me_2SiCp''[(–)-menthylCp]LnCH(TMS)$_2$ complexes (Table 2, entries

(21) (a) Bakos, J.; Tóth, I.; Heil, B.; Markó, L. *J. Organomet. Chem.* **1985**, *279*, 23–29. (b) Hayashi, T.; Tanaka, M.; Ogata, I. *Tetrahedron Lett.* **1977**, *18*, 295–296.

(22) Halterman, R. C. *Chem. Rev* **1992**, *92*, 965–994.

(23) Based upon $[\alpha]^{20}D$ = +28.4° for (*S*)-(+)-2-phenylbutane (c = 1.00, 95% EtOH, l = 0.5 dm);[24] rotation confirmed by independent synthesis (see Experimental Section) from (*S*)-(+)-2-phenylbutyric acid.[25] Reported ee values based upon lower [α] values must be adjusted downward accordingly.

(24) Lardicci, L.; Menicagli, R.; Salvadori, P. *Gass. Chim. Ital.* **1968**, *98*, 738–759.

(25) Elsenbaumer, R. L.; Mosher, H. S. *J. Org. Chem.* **1979**, *44*, 600–604.

19 and 29). Interestingly, under non-mass-transport-limited conditions (i.e., a rapid, non-H_2-starved stirring regime), the diastereomerically-pure (*R*)-Me_2SiCp''[(+)-neomenthylCp]SmCH(TMS)$_2$ precatalyst leads to a *higher* and *opposite* product enantioselectivity (73% ee (*R*)) than (*S*)-Me_2SiCp''[(+)-neomenthylCp]SmCH(TMS)$_2$ (19% ee (*S*)) for 2-phenyl-1-butene hydrogenation (entries 9, 13). These results underscore the diastereomeric character of these pseudoenantiomorphous catalysts which differ significantly in sign and efficiency of chirality transfer and also turn over at different rates (5700 h^{-1} versus 4000 h^{-1}, respectively, *vide infra*). Interestingly, when the same reduction is carried out under the same conditions with the mixed 1:1 (*R,S*)-Me_2SiCp''-[(+)-neomenthylCp]SmCH(TMS)$_2$ precatalyst, the observed N_t is close to the average of the values quoted above (5000 h^{-1} observed vs 4850 h^{-1} calculated), and the observed ee is close to the average of the aforementioned transformations, weighted by the respective N_t values (46% ee (*R*) observed vs 35% ee (*R*) calculated). Noteworthy here is the absence of large nonlinear effects[26] in the asymmetric induction (under non-mass-transport-limited conditions), which argues that the (*R*) and (*S*) catalyst units are not transferring chirality cooperatively (or anticooperatively) in a multimolecular fashion. Evidence that (–)-menthyl (*R*) and (*S*) catalyst epimers also yield hydrogenation products of opposite chirality but with unequal enantioselectivity is provided by entries 20 and 25 of Table 2. It will be seen in more detail in kinetic studies (*vide infra*) that the (*R*)-, (*S*)-, and (*R,S*)-organosamarium precatalysts obey the same rate law but exhibit different turnover frequencies and selectivities.

The catalytic deuteration of styrene was also investigated with precatalysts (*R*)-**6f** and 70/30 (*S*)/(*R*)-**6f**. Each catalyst preferentially selects the opposite enantioface of styrene, yielding ethylbenzenes of composition 43% (*R*) and 72% (*S*), respectively (Table 2). For a given precatalyst, the selectivity is higher for styrene than for α-ethylstyrene, with atom transfer to the same enantioface. This suggests that similar but increased steric discrimination (i.e., H vs Et in the α position of styrene) is a significant component of asymmetric induction. The exclusive formation of ethylbenzene-1,2-d_2 argues that β-hydride elimination/readdition does not effectively compete with hydrogenolysis of the intermediate Ln alkyl formed by olefin insertion.

As noted earlier, the rapidity of the hydrogenations at higher temperatures necessitates the use of rapid stirring (vortex mixer) to avoid mass-transfer (H_2 starvation) effects on kinetic measurements. Effects on enantioselection were also investigated. As can be seen in Table 2, the magnitudes of the mass-transfer effects (normal rapid stirring versus vortex) vary, ranging from near-negligible for homochiral (*R*)- and (*S*)-(+)-neomenthyl catalysts (2% ee, entries 8, 9; 2% ee, entries 14, 15) and (*R*)-(–)-menthyl catalysts (8% ee, entries 19, 20) to more substantial for comparisons involving mixed catalysts (16% ee, entries 24, 25; 27% ee, entries 3, 4). The reason for the greater sensitivity of the latter two systems is not immediately obvious, although it may reflect, among other subtle factors, differential β-H elimination versus hydrogenolysis rates (*vide infra*).

Variable-temperature studies of the asymmetric hydrogenation indicate that enantioselectivities *increase* as the the temperature decreases (Table 2, entries 4–7, 9–12, 13–16, 20–23, 25–28). Analyzing these data in a modified Eyring format (eq 11)[27] yields relatively smooth plots (Figure 4) with no obvious inversions,

$$\ln p = \frac{\Delta\Delta H}{RT} + \frac{\Delta\Delta S}{R} \qquad p = \frac{k(\text{major product})}{k(\text{minor product})} \quad (11)$$

which might be taken as mechanistic evidence for sequential steps

(26) (a) Evans, D. A.; Nelson, S. G.; Gagné, M. R.; Muci, A. R. *J. Am. Chem. Soc.* **1993**, *115*, 9800–9801. (b) Noyori, R.; Kitamura, M. *Angew. Chem., Int. Ed. Engl.* **1991**, *30*, 49–69. (c) Puchot, C.; Samuel, O.; Dunach, E.; Zhao, S.; Agami, C.; Kagan, H. B. *J. Am. Chem. Soc.* **1986**, *108*, 2353–2357.

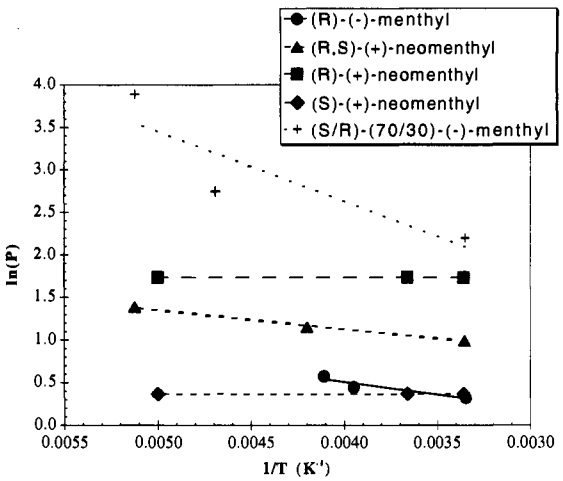

Figure 4. Erying plots for product enantiomeric excesses in the hydrogenation of 2-phenyl-1-butene using the chiral precatalysts indicated. Lines represent least-squares fits to eq 11.

Table 3. Eyring Parameters for the Asymmetric Catalytic Hydrogenation of 2-Phenyl-1-butene Mediated by Chiral Organosamarium Complexes[a]

precatalyst	precatalyst structure	$\Delta\Delta H^{\ddagger}$ (kcal/mol)	$\Delta\Delta S^{\ddagger}$ (eu)
(*R,S*)-**6e**	(*R,S*)-neomenthylSmCH(TMS)$_2$	0.43(6)	0.6(1)
(*R*)-**6c**	(*R*)-neomenthylSmCH(TMS)$_2$	0.0(1)	3.3(4)
(*S*)-**6c**	(*S*)-neomenthylSmCH(TMS)$_2$	0.0(1)	2.9(3)
(*R*)-**6f**	(*R*)-menthylSmCH(TMS)$_2$	0.8(1)	1.4(2)
(70/30) (*S*/*R*)-**6f**	(*S*/*R*)-menthylSmCH(TMS)$_2$	1.6(7)	1.3(6)

[a] Fit by least-squares to eq 12.

in enantioselection.[27] Derived Eyring parameters from least-squares fits to these data are compiled in Table 3. With the exception of the 70/30 (*S*)/(*R*)-**6f** data, which no doubt represent a composite, the $\Delta\Delta H^{\ddagger}$ and $\Delta\Delta S^{\ddagger}$ parameters appear to be rather small compared to other asymmetric catalytic hydrogenation systems.[27]

Kinetics of Organolanthanide-Catalyzed Enantioselective Hydrogenation. The kinetics of the asymmetric hydrogenation with (*S*)-, (*R*)-, and (*R,S*)-**6c** and (*R*)- and (**70/30**) (*S*/*R*)-**6f** were studied under non-mass-transport-limited (high-speed agitation) conditions to obtain intrinsic turnover frequencies and to establish the catalytic rate law. A thermostated, constant pressure (pseudo-zeroth-order in H_2 pressure), efficient convection batch reactor[6a] was employed. The time dependence of the hydrogen uptake was monitored as a function of the total Ln and olefin concentrations as well as hydrogen pressure. For the aforementioned chiral organosamarium complexes, the rate law of eq 12 is obtained under the present non-mass-transport-limited conditions[28] at 25.0 ± 0.2 °C. Typical kinetic plots for olefin consumption as a function

$$v = k[\text{Ln}]^{1/2}[\text{olefin}]^{0}[H_2]^{1} \quad (12)$$

of precatalyst concentration and hydrogen pressure (Figures 5 and 6) clearly indicate a zeroth-order dependence of the catalytic rate on olefin concentration. Experiments in which the initial concentrations of (–)-menthyl and (+)-neomenthyl organosa-

(27) (a) Göbel, T.; Sharpless, K. B. *Angew. Chem., Int. Ed. Engl.* **1993**, *32*, 1329–1331. (b) Buschmann, H.; Scharf, H.-D.; Hoffmann, N.; Esser, P. *Angew. Chem., Int. Ed. Engl.* **1991**, *30*, 477–515 and references therein. (c) It is reasonably assumed that mass transfer effects on ee attenuate with falling temperatures.

(28) The present conditions for kinetic measurements represent those which are catalytically meaningful and experimentally practicable. It is not inconceivable that the present range of olefin concentrations encompasses a "saturation" regime and that first-order kinetics in olefin might be observed if *exceedingly low* olefin and catalyst concentrations (a regime where poisoning by trace O_2, H_2O, etc. becomes a major concern) were employed and the rate of H_2 uptake could be accurately measured under such conditions.

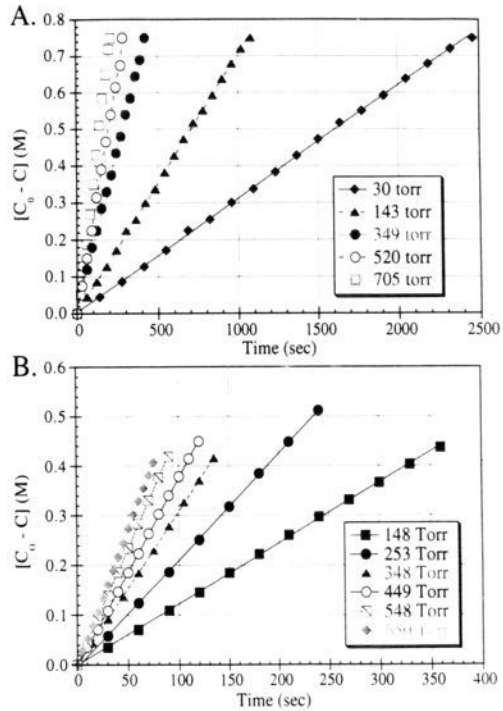

Figure 5. Plot of normalized [substrate(A_0) – substrate(A_t)] for the catalytic hydrogenation of 2-phenyl-1-butene as a function of time at various total hydrogen pressures at constant initial precatalyst concentration catalyzed by (A) (*R*)-Me_2SiCp''[(–)-menthylCp)SmCH(TMS)$_2$ [(*R*)-**6f**] and (B) (*S*,*R*)-Me_2SiCp''[(+)-neomenthylCp]SmCH(TMS)$_2$ [(*R*,*S*)-**6c**].

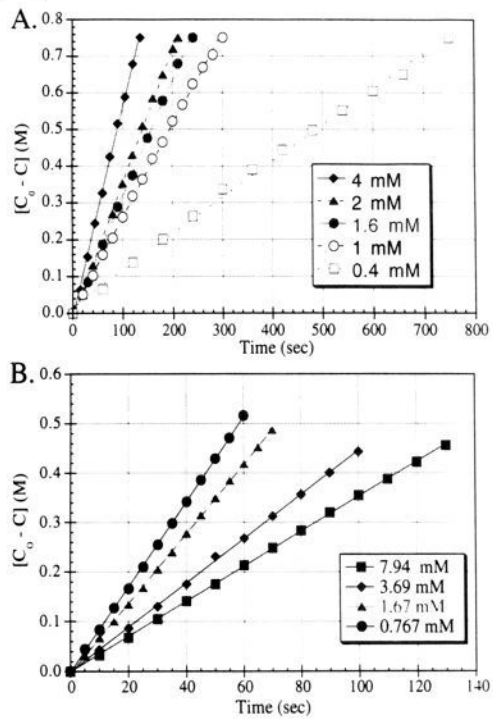

Figure 6. Plot of normalized [substrate(A_0) – substrate(A_t)] for the catalytic hydrogenation of 2-phenyl-1-butene as a function of time at various total precatalyst concentrations and constant total hydrogen pressure (750 Torr) catalyzed by (A) (*R*)-Me_2SiCp''[(–)-menthylCp]-SmCH(TMS)$_2$ [(*R*)-**6f**] and (B) (*S*,*R*)-Me_2SiCp''[(+)-neomenthylCp]-SmCH(TMS)$_2$ [(*R*,*S*)-**6c**].

marium hydrocarbyls **6c** and **6f**, respectively, were varied from 0.51 to 8.04 mM indicate a reaction order of 0.5 ± 0.1 in total lanthanide concentration at constant hydrogen pressure (Figure

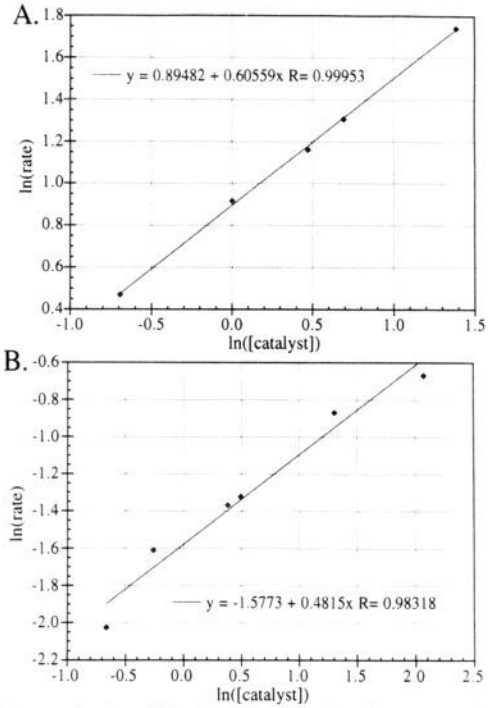

Figure 7. Determination of kinetic order in lanthanide concentration for the asymmetric hydrogenation of 2-phenyl-1-butene catalyzed by (A) (*R*)-Me_2SiCp''[(–)-menthylCp]SmCH(TMS)$_2$ [(*R*)-**6f**] and (B) (*S*,*R*)-Me_2SiCp''[(+)-neomenthylCp]SmCH(TMS)$_2$ [(*R*,*S*)-**6c**]. Catalyst concentrations are in mM.

7). The turnover frequency depends on the total Ln concentration, with a maximum (N_t = 26 000 h^{-1}) observed with **6c** for [Ln] = 0.40 mM and P_{H_2} = 1 atm. However, below this threshold Ln concentration, N_t declines, and hydrogen uptake/time curves deviate significantly from linearity. This suggests that poisoning by trace impurities (*e.g.*, H_2O,O_2) begins to dominate at very low Ln concentrations and high substrate:catalyst ratios (>900:1). In all cases, N_t at constant catalyst concentration depends in a first-order manner on total hydrogen pressure over the 75–705 Torr range (Figure 8). Significant kinetic isotope effects (KIEs) of k_{H_2}/k_{D_2} = 1.5–2.3 are also observed (Table 2).

It is also found that N_t for 2-phenyl-1-butene hydrogenation catalyzed by (*R*,*S*)-**6c** (N_t = 5000 h^{-1}) is approximately 5× greater than that for the (achiral) (Cp′$_2$SmH)$_2$-catalyzed process (N_t = 1100 h^{-1}) at similar total lanthanide concentrations ([Ln]$_{total}$ = 8.0 mM) and hydrogen pressures (650 Torr). However, unlike (*R*,*S*)-**6c**-catalyzed hydrogenation, the kinetics for (Cp′$_2$SmH)$_2$-catalyzed hydrogenation display a clear first-order dependence on olefin concentration, supporting a turnover-limiting olefin insertion step. These observations suggest an effectively more open lanthanide coordination sphere in the chiral catalysts, logically a consequence of linked cyclopentadienyl ligands and deleted ring substituents. The derived rate constants (Table 4) for asymmetric hydrogenation, k = 20.7–35.4 M$^{-1/2}$ s^{-1}, indicate quantitatively that hydrogenation is rapid, which is especially noteworthy in view of the enantiomeric excesses observed.

Discussion

Catalytic Asymmetric Hydroamination/Cyclization. Kinetics, Mechanism, and Origin of Enantioselection. The basic mechanism for the present asymmetric amino olefin hydroamination/cyclization by chiral organolanthanide classes **6** and **7** appears to be analogous to the mechanism proposed for the achiral Cp′$_2$-Ln-catalyzed process (Scheme 2).[9] The precatalysts Cp′$_2$LnE(TMS)$_2$ (E = CH, N) undergo rapid protonolysis of the Ln–E bond by the substrate, forming a labile amine–amido adduct which

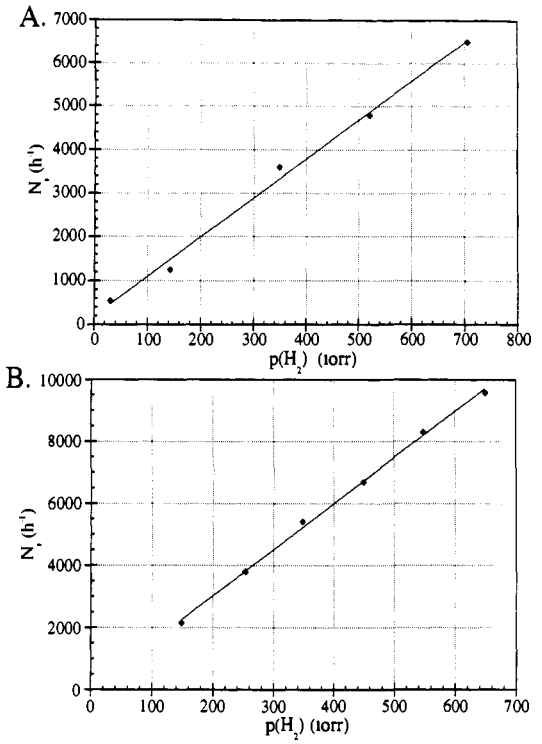

Figure 8. Dependence of the turnover frequency (N_t) on hydrogen pressure for the asymmetric hydrogenation of 2-phenyl-1-butene catalyzed by (A) (*R*)-Me_2SiCp''[(–)menthylCp]SmCH(TMS)$_2$ [(*R*)-**6f**] and (B) (*S*,*R*)-Me_2SiCp''[(+)-neomenthylCp]SmCH(TMS)$_2$ [(*R*,*S*)-**6c**].

Table 4. Kinetic Data for the Asymmetric Catalytic Hydrogenation of 2-Phenyl-1-butene Mediated by Chiral Organosamarium Complexes

precatalyst	precatalyst structure	k^a	N_t $(h^{-1})^c$
(*S*)-**6c**	(*S*)-neomenthylSmCH(TMS)$_2$	0.115(2)	4000
(*R*)-**6c**	(*R*)-neomenthylSmCH(TMS)$_2$	0.166(3)	5700
(*R*,*S*)-**6c**	(*R*,*S*)-neomenthylSmCH(TMS)$_2$	0.143(1)	5000
(*R*)-**6f**	(*R*)-menthylSmCH(TMS)$_2$	0.097(2)	3400
(70/30) (*S*/*R*)-**6f**	(*S*/*R*)-menthylSmCH(TMS)$_2$	0.154(3)	5300
(*S*)-**6f**	(*S*)-menthylSmCH(TMS)$_2$	0.178[b]	
Cp'_2SmCH(TMS)$_2$			1100

[a] Rate law, $v = k[M]^{1/2}[H_2]^1$, in units of $M^{1/2}$ s^{-1} atm^{-1}. Multiply by 213 to convert to $M^{-1/2}$ s^{-1}. [b] Calculated. [c] $[Ln]_T$ = 8.0 mM; P_{H_2} = 650 Torr.

undergoes rapid bound amine–amide exchange as well as rapid bound–free amine exchange. Turnover-limiting intramolecular olefin insertion into the Ln–N bond (i) and subsequent rapid intra- or intermolecular protonolysis of the resulting Ln–C bond afford product heterocycle (ii) and regenerate the catalyst. The present zeroth-order or near-zeroth-order dependence on substrate concentration of the initial Me_2SiCp''(R*Cp)LnR-mediated cyclization rates is consistent with this scenario.

Chiral complexes **6** and **7** exhibit significant rate enhancements for hydroamination/cyclization compared to the aforementioned achiral Cp'_2Ln complexes. For the cyclization of 1-aminopent-4-ene at 25 °C in toluene, the turnover frequency increases approximately 1 order of magnitude from $Cp'_2SmCH(SiMe_3)_2$ (N_t = 6 h^{-1}) to (*R*)-**6c**/**7b** (N_t = 62 h^{-1}), reasonably suggesting less steric congestion in the catalyst equatorial "girdle" (plane bisecting the ring centroid–Sm–ring centroid angle) of the latter complex. A similar relationship between N_t and ancillary ligation-based Ln unsaturation is observed in the cyclization of 2,2-dimethyl-1-aminopent-4-ene at 80 °C, where the rate increases in the order $Cp'_2LuCH(SiMe_3)_2$ (N_t < 1 h^{-1}), $Me_2SiCp''_2LuCH(SiMe_3)_2$ (N_t = 75 h^{-1}), $Et_2SiCp''CpLuCH(SiMe_3)_2$ (N_t = 200 h^{-1}).[9c] In general, N_t decreases with decreasing metal ionic radius for both Cp'_2Ln catalysts and chiral catalysts, while substrate structure–N_t patterns are also similar.

Scheme 2. Simplified Scenario for Organolanthanide-Catalyzed Hydroamination

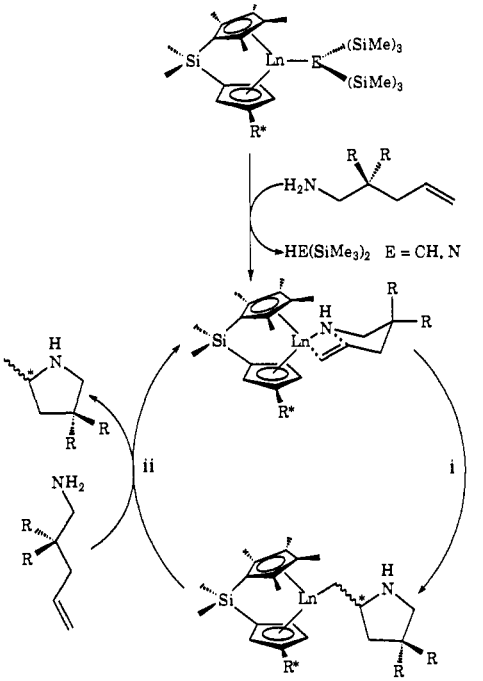

In situ ^{1}H NMR monitoring of the asymmetric hydroamination/cyclization process indicates rapid generation of a common organometallic structure under the catalytic conditions, corresponding to an amine–amido adduct.[1,9c] Although initial Ln–C/Ln–N protonolysis proceeds rapidly and with retention of configuration at the Ln center, *in situ* ^{1}H NMR also indicates that the catalysts undergo epimerization in the presence of excess amine at rates comparable to those of catalytic turnover.[1] Thus, it is not surprising that both epimers of a particular precatalyst yield heterocyclic products of the same sign and approximately the same ee in preparative scale reactions (*vide supra*, Table 1). Where comparative data are available, note (Table 1, entries 6 + 7, 22 + 23) that catalysts of opposite configuration do not exhibit identical *initial* turnover frequencies. This is not surprising in view of their diastereomeric relationship, and further comments regarding these effects will be made in the discussion of hydrogenation (*vide infra*). That these catalysts readily undergo epimerization under catalytic conditions and that equilibrium between catalyst epimers is established well before complete substrate consumption in preparative scale reactions convey interesting implications. Since equilibrium epimer ratios are frequently far from 1:1, this process does not necessarily destroy catalyst homochirality but in fact can, in many cases, permit the successful utilization of stereochemically *impure* catalysts. Furthermore, it should be possible to "preepimerize" catalysts with a volatile (readily removed) amine prior to addition of the hydroamination/cyclization substrate.

In regard to enantioselection, stereochemical interpretation of the present results is complicated somewhat by epimerization of the precatalysts and the universal proviso that relative product populations may not always parallel relative catalyst populations.[29] Nevertheless, several generalizations appear reasonable. From Table 1, note that, with the exception of the small Lu^{3+} ion,

(29) Halpern, J. In *Asymmetric Synthesis*; Morrison, J. D., Ed.; Academic Press: New York, 1985; Vol. 5, Chapter 2, and references therein.

(+)-neomenthyl-based catalysts produce an excess of (*R*)-(−) heterocyclic product, while (−)-menthyl- and (−)-phenylmenthyl-based catalysts produce an excess of (*S*)-(+) product. The Lu^{3+} result is always opposite, with a modest ee. Assuming that the epimerization results with *n*-propylamine[1] are representative of other primary amines such as the amino olefin substrates, then it can be anticipated that under steady-state catalytic conditions, the (+)-neomenthyl-based catalysts will be predominantly in the (*R*) configuration, while the (−)-menthyl- and (−)-phenylmenthyl-based catalysts will be in the (*S*). Hence, an excess of (*R*) product correlates with enrichment in (*R*) catalyst epimer, and an excess of (*S*) product correlates an excess of (*S*) catalyst epimer.

Studies of both the achiral and chiral amino olefin hydroamination/cyclization systems indicate that the irreversible, turnover-limiting (and presumably stereodifferentiating) olefin insertion process (Scheme 2, step i) is sterically sensitive, as evidenced by the aforementioned metal ancillary ligand and substrate effects, as well as highly organized ($\Delta S^{\ddagger} = -19$ eu).[9c] Thus, nonbonded repulsive interactions are expected to play a significant role in enantioselection. From what is known about 1,5 insertive olefin cyclization processes in d^0/f^n metallocene coordination spheres,[2,30] seven-membered chairlike transition states are likely in the present case. Assuming such a reaction coordinate, there are four reasonable trajectories possible for insertive olefin approach to the Ln center. The olefinic functionality may approach along the central ring-centroid–Ln–ring centroid bisector ("frontally", eqs 13 and 14) or approximately perpendicular to this direction ("laterally"), from the side distal to the bulky R* group (eqs 15 and 16). For each mode (frontal or lateral) of insertion, one of

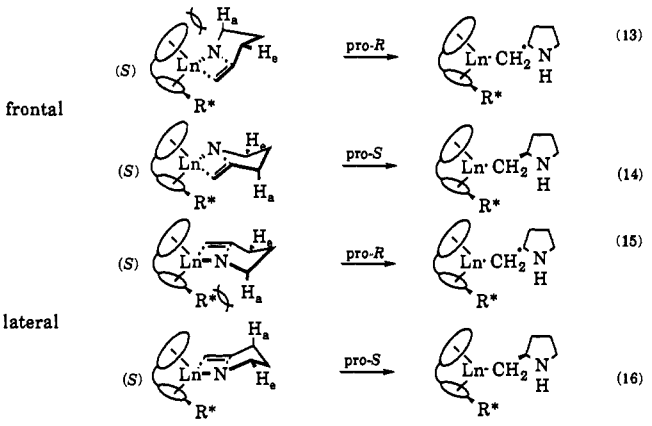

the trajectories involves unfavorable steric interactions between axial substituents of the transition state and either the methyl substituents of the Cp″ (eq 13) or the R* auxiliary (eq 15). Thus, for the (*S*) catalyst configuration, the *pro-S* approach is favored for *either mode* of olefin insertion. Similarly, the (*R*) catalyst configuration should favor formation of the (*R*) antipode of product in either mode. Similar arguments have been made to rationalize diastereoselectivity in the cyclization of 2-aminohex-5-ene to *trans*-2,5-dimethylpyrrolidine with achiral organolanthanide precatalysts.[9c,31] For the present asymmetric transformations, product configurations can reasonably exclude two of the four possibilities in eqs 13–16. The importance here of a seven-membered cyclic transition state in the stereodifferentiating step is further argued by the diminished ee values and *identical* product absolute configurations in cyclization of aminohexene **10** using (*R*)-**6c**/**7b** and (*S*)-**6f**/**7e** as precatalysts (Table 1, entries 33 and 34). This substrate would require an eight-membered transition state of greater conformational mobility and differing steric demands. As already noted, the selectivity effected by the sterically congested Lu^{3+} complexes is opposite that of the larger lanthanides, although the (−)-menthyl catalyst and the (+)-neomenthyl catalyst invariably select for opposite antipodes of product. This observation suggests that additional steric factors intervene as the Ln^{3+} radius decreases.

The enantioselective hydroamination/cyclization process represents a direct method of catalytically forming C–N bonds with relatively high asymmetric induction. The scope of this process may well be extendable in terms of applicable substrates, similar to the Cp'_2Ln-catalyzed processes,[9] and is a potentially useful approach to important heterocyclic nitrogen compounds.[32,33] Potential generality, large turnover capacity, high product value, and ability to select for either product enantiomer are attractive features.

Catalytic Enantioselective Olefin Hydrogenation. Kinetics and Mechanism. The chiral organolanthanide hydrocarbyl complexes serve as effective precatalysts for the asymmetric hydrogenation of 2-phenyl-1-butene and the deuteration of styrene with high efficiency and enantioselectivity. Enantioselection depends on the efficiency of chirality transfer from the catalyst to the substrate, which is mechanistically determined by the nature of the microscopic catalyst–substrate interaction. The analogous achiral process for simple linear and cyclic alkenes catalyzed by $(Cp'_2LnH)_2$ and $(Me_2SiCp''_2LnH)_2$ complexes has been studied in some detail (Scheme 3).[6a] The proposed mechanism involves initial olefin insertion into a Ln–H bond (step i) of the reactive "Cp'_2LnH" monomer in equilibrium with a dimer (K_{eq}), forming an organolanthanide hydrocarbyl. Subsequent hydrogenolysis of the Ln–C bond of this intermediate (step ii) regenerates the active "Cp'_2LnH" complex with concomitant liberation of alkane. Two limiting kinetic regimes have been identified under typical catalytic conditions: turnover-limiting hydrogenolysis ($k_i > k_{ii}$) and turnover-limiting olefin insertion ($k_i < k_{ii}$). The first scenario usually obtains for simple α-olefins (e.g., 1-hexene) and is described by a rate expression zeroth-order in substrate, first-order in Ln, and first-order in P_{H_2} (eq 17). Here, olefin capture

$$v = k[\text{olefin}]^0[\text{lanthanide}]^1[H_2]^1 \qquad (17)$$

(insertion) by the metal hydride is rapid and irreversible, essentially displacing the hydride equilibrium entirely to alkyl (demonstrated in stoichiometric reactions), while Ln–C hydrogenolysis is turnover-limiting. The second scenario obtains for more sterically hindered internal olefins (e.g., cyclohexene), and the rate depends linearly on the olefin concentration (eq 18), is half-order in Ln, and zeroth-order in P_{H_2}. Here, the dimeric

$$v = k[\text{olefin}]^1[\text{lanthanide}]^{1/2}[H_2]^0 \qquad (18)$$

hydride[4,6] is involved in a rapid preequilibrium with a reactive monomer, olefin capture is turnover-limiting, and hydrogenolysis follows this slow step. In the present study, it is found that the hydrogenation of 2-phenyl-1-butene catalyzed by *achiral* (Cp'_2-

(30) Chairlike transition states have been postulated for other 1,5-cyclizations on d^0 configuration Cp_2MR_n ($n = 1$–2) complexes: (a) Resconi, L.; Waymouth, R. W. *J. Am. Chem. Soc.* **1990**, *112*, 4953–4954. (b) Clawson, L.; Soto, J.; Buchwald, S. L.; Steigerwald, M. L.; Grubbs, R. H. *J. Am. Chem. Soc.* **1985**, *107*, 3377–3378. (c) Bunel, E.; Burger, B. J.; Bercaw, J. E. *J. Am. Chem. Soc.* **1988**, *110*, 976–978. (d) Piers, W. E.; Bercaw, J. E. *J. Am. Chem. Soc.* **1990**, *112*, 9406–9407. (e) Cavallo, L.; Guerra, G.; Corrandini, P.; Resconi, L.; Waymouth, R. M. *Macromolecules* **1993**, *26*, 260–267. (f) Coates, G. W.; Waymouth, R. W. *J. Am. Chem. Soc.* **1993**, *115*, 91–99.

(31) These simplified arguments, of course, ignore any steric effects exerted by labile substrate molecules which may also be in the coordination sphere.[9c]

(32) For examples of the synthetic utility of *trans*-**14**, see: (a) Porter, N. A.; Scott, D. M.; Rosenstein, I. J.; Giese, B.; Veit, A.; Zeitz, H. G. *J. Am. Chem. Soc.* **1991**, *113*, 1791–1799. (b) Giese, B.; Zehnder, M.; Roth, M.; Zietz, H. *J. Am. Chem. Soc.* **1990**, *112*, 6741–6742. (c) Schlessinger, R. H.; Iwanowicz, E. J.; Springer, J. P. *J. Org. Chem.* **1986**, *51*, 3070–3073.

(33) For leading references on natural products containing similar nitrogen heterocycles, see: (a) *The Alkaloids: Chemistry and Pharmacology*; Brossi, A., Cordell, G. A., Eds.; Academic: New York, 1992. (b) *Alkaloids: Chemical and Biological Perspectives*; Pelletier, S. W., Ed.; Wiley-Interscience: New York, 1988. (c) Belen'kii, L. I. In *Advances in Heterocycle Chemistry*; Katritsky, A. R., Ed.; Academic: New York, 1988; Vol. 44, Chapter 4. (d) *Comprehensive Heterocyclic Chemistry*; Meth-Coba, O., Ed.; Pergamon: New York, 1984.

Scheme 3. Mechanism for Bis(pentamethylcyclopentadienyl)organolanthanide-Catalyzed Olefin Hydrogenation

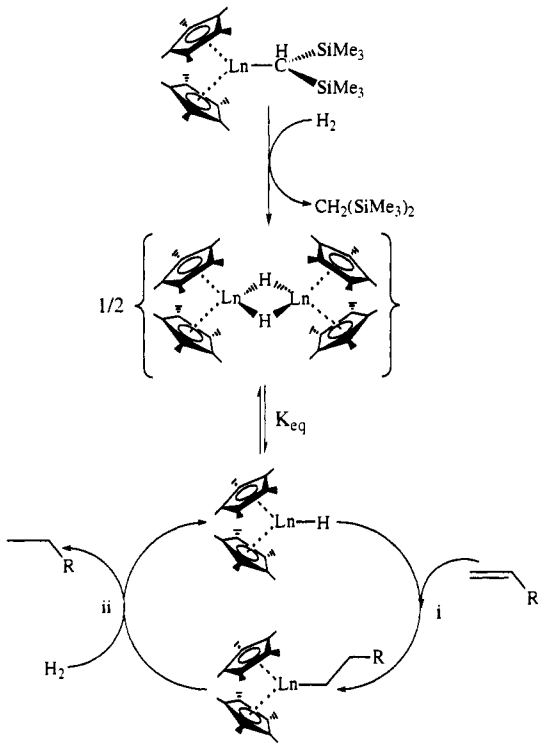

Scheme 4. Proposed Mechanism for Asymmetric Olefin Hydrogenation with Chiral Organolanthanides

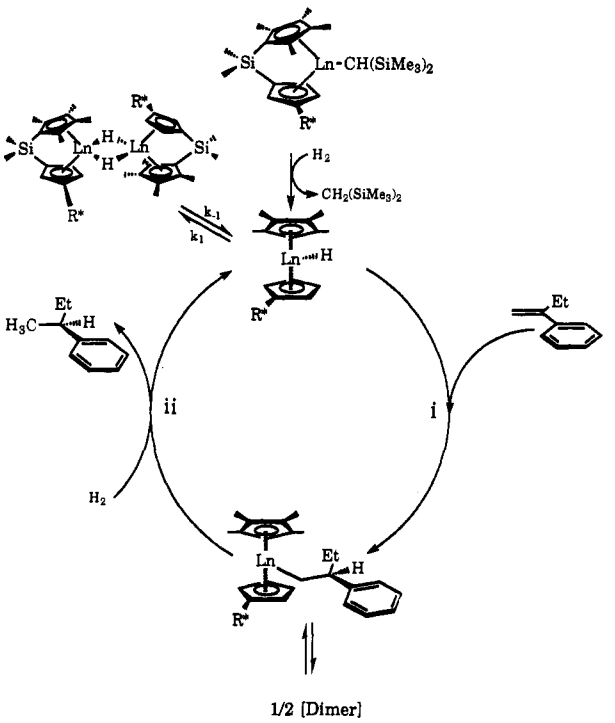

SmH)$_2$ obeys the latter rate expression (eq 18), and olefin insertion is turnover-limiting. In contrast, the kinetics for 2-phenyl-1-butene hydrogenation with precatalysts **6c** and **6f** display first-order dependence on P_{H_2}, zeroth-order dependence on olefin concentration, and half-order dependence on Ln concentration (eq 12), supporting turnover-limiting hydrogenolysis. Indeed, the observed KIEs for deuteration of 2-phenyl-1-butene, k_{H_2}/k_{D_2} = 1.5–2.3 (Table 2) are consistent with observed isotope effects for the hydrogenolysis of metal–alkyl bonds of other d^0/f^n complexes in solution[34] and on metal oxide supports.[35] In addition, N_t for 2-phenyl-1-butene hydrogenation is significantly greater for (*R*,*S*)-**6c** (5000 h^{-1}) as a precatalyst than for (Cp′$_2$SmH)$_2$ (1100 h^{-1}) at P_{H_2} = 650 Torr and comparable total organolanthanide concentrations ([Ln] = 8.0 mM). These observations suggest a lesser degree of steric congestion at the present Me$_2$SiCp″(R*Cp)Ln centers and are consistent with existing structure/reactivity data supporting a general increase in reactivity upon opening of the Ln coordination sphere about the equatorial girdle.[6,7,36]

As indicated above, the 2-phenyl-1-butene asymmetric hydrogenation kinetics do not conform to either of the limiting kinetic scenerios of (Cp′$_2$LnH)$_2$-catalyzed hydrogenations. Zeroth-order dependence on olefin suggests rapid, effectively irreversible olefin capture[28] prior to the turnover-limiting step, while half-order dependence on Ln concentration suggests a reversible preequilibrium involving dissociation of a dialkyl or hydridoalkyl dimer preceding turnover-limiting hydrogenolysis. In regard to the catalytic importance of the reversible dissociation involving a *dihydride dimer*, catalyst solutions after exhaustion of olefin are identical by NMR to independently prepared solutions of the hydride complexes. However, they are much less active for olefin hydrogenation than either (Cp′$_2$LnH)$_2$ solutions or the initial catalyst solutions generated by *in situ* hydrocarbyl hydrogenolysis in the presence of excess olefin. The reactivity of the ultimate chiral hydrido complexes thus resembles that of (Me$_2$SiCp″CpLnH)$_2$ (Ln = Y, Lu; R = Me, Et) complexes, which are unreactive toward olefin hydrogenation due to rearrangement to a "ring-spanning" structure (**A**).[8] This renders the complexes incapable of dissociation to form reactive monomers, unlike (Cp′$_2$LnH)$_2$ and (Me$_2$SiCp″$_2$LnH)$_2$.[6] Significantly, the degree of cyclopentadienyl ring substitution in the present chiral complexes more closely approaches less-substituted R$_2$SiCp″CpLnCH(SiMe$_3$)$_2$ than Me$_2$SiCp″$_2$LnCH(SiMe$_3$)$_2$. Although epimerization of the organolanthanide chloro complexes in donor solvents and classes **6** and **7** in the presence of excess amine supports the lability of the Ln–CpR* interaction, analogous epimerization is not observed upon hydrogenolysis of the hydrocarbyls nor in solutions of the resulting hydrides.[1] Taken together, these observations suggest that the lanthanide hydride dimer is probably not a ring-spanning dimer but is a tightly associated ($k_1 \gg k_{-1}$) μ-H dimer (e.g., eq 19)which, however, is too unreactive to play a major role in the

$$2\mathrm{Me_2SiCp''(R^*Cp)Ln\text{-}H} \underset{k_{-1}}{\overset{k_1}{\rightleftharpoons}} [\mathrm{Me_2SiCp''(R^*Cp)LnH}]_2 \quad (19)$$

catalytic cycle. Efforts to grow crystals of these hydrides suitable for diffraction studies have so far been unsuccessful.

A tentative scenario for the hydrogenation of 2-phenyl-1-butene using precatalysts **6** is presented in Scheme 4. Initial hydrogenolysis of the LnCH(TMS)$_2$ bond of the precatalyst generates a transient monomeric hydride which rapidly undergoes olefin insertion (i).[37] The resulting alkyl then undergoes hydrogenolysis in a turnover-limiting step (ii), affording alkane and regenerating the hydride. Additionally, the intermediate alkyl must be in rapid equilibrium with a dimer according to the observed rate law. The exact nature of this dimer has not been elucidated, although reasonable structures may be postulated in analogy to known chemistry. A doubly-bridging alkyl dimer has precedent in (Cp$_2$-

(34) Lin, Z.; Marks, T. J. *J. Am. Chem. Soc.* **1987**, *109*, 7979–7985 and references therein.

(35) Gillespie, R. D.; Burwell, R. J., Jr.; Marks, T. J. *Langmuir* **1990**, *6*, 1465–1477.

(36) (a) Fendrick, C. M.; Mintz, E. A.; Schertz, L. D.; Marks, T. J.; Day, V. W. *Organometallics* **1984**, *3*, 819–821. (b) Fendrick, C. M.; Schertz, L. D.; Day, V. W.; Marks, T. J. *Organometallics* **1988**, *7*, 1828–1830.

(37) The insertion is portrayed here as a "1,2" insertion process (Ln delivered to C(β)) on the basis of steric considerations. However, the present data are also compatible with a "2,1" insertion, which places the electrophilic Ln^{3+} in closer proximity to the arene π electron system.

$Ln)_2(\mu\text{-}R)_2$ complexes.[38] The alkyl bridging mode might even incorporate arene π coordination similar to that of the styrene complex $(Cp'_2Sm)_2(\mu\text{-}\eta^2\text{:}\eta^4\text{-}CH_2CHPh)$ (**B**).[39] In this case, the

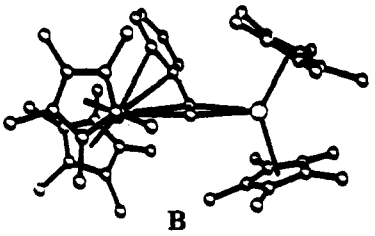

B

increase in ee with increasing Ln^{3+} radius might reflect the facility with which the larger Ln ions can accommodate this multihapto structure. Another possibility is a μ-hydrido/μ-alkyl dimer such as $(Cp'_2Ln)_2(\mu\text{-H})(\mu\text{-R})$. Structurally similar $R_2SiCp''CpLuCH(SiMe_3)_2$ (R = Me, Et) undergoes partial hydrogenolysis to form a structure assigned from NMR as $(Me_2SiCp''CpLu)_2(\mu\text{-H})[\mu\text{-}CH(SiMe_3)_2]$, a marginally active catalyst for 1-hexene hydrogenation (N_t = 21 h^{-1}).[8] In this case, formation of the unreactive, ring-spanned hydride dimer ultimately terminates catalytic activity. In the presence case, it appears that a tightly associated μ-H dimer accounts for the greatly diminished catalytic activity of the preformed hydrides (*vide supra*). The coordinatively unsaturated, C_2-symmetric Y complex $(Me_2Si[1\text{-}TMS\text{-}3\text{-}t\text{-}BuCp]_2YH)_2$ exhibits similar behavior,[40a] with *in situ* generated hydrido species being far more reactive than preformed hydrides. ^1H NMR indicates that this complex does not undergo ligand redistribution to produce a ring-spanning dimer at significant rates.[40b] It thus appears that for coordinatively unsaturated organolanthanides, $k \gg k_{-1}$ (in eq 19).

Enantioselection in asymmetric catalytic transformations is usually fixed in the first irreversible step involving a diastereomeric transition state.[41] In the present hydrogenation, it is reasonable that the enantioselective step is olefin insertion into the Ln–hydride bond. Under non-mass-transport-limited conditions, insertion is probably operationally irreversible since thermodynamic data indicate $\Delta H \approx -20$ kcal/mol,[42] and the rate constant for olefin insertion (k_1) should be quite large since the turnover-limiting hydrogenolysis step is rapid under these conditions (k = 20.7–35.4 $M^{-1/2}\,s^{-1}$). The exothermicity of insertion also argues that the structure of the transition state is reactant-like.[43] However, it appears that β-hydride elimination can become kinetically accessible under conditions of H_2 starvation encountered in the H_2 diffusion-controlled (slow stirring speed) regime. In this situation, β-elimination could partially scramble the initial stereoselection of insertion by equilibrating stereoisomers of the intermediate alkyl (e.g., eq 20), where the intermediate may involve either bound or free olefin. Permutation of LnR

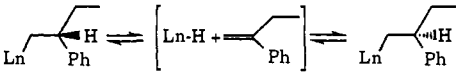

(20)

stereoisomers via this process could account for the small but reproducible erosion in enantioselection under H_2 mass-transfer-limited conditions—from 16% (*R*) to 8% (*R*) and from 80% (*S*) to 64% (*S*), for (–)-menthyl catalysts derived from (*R*)-**6f** and (70/30 (*S*)/(*R*)-**6f**, respectively (Table 2, entries 19 + 20, 24 + 25). In contrast, hydrogenations using catalysts derived from (+)-neomenthyl precatalysts (*R*)-**6c** and (*S*)-**6c** do not exhibit a significant degradation (≤6%) in ee under H_2 mass-transfer-limited conditions (Table 2, entries 8 + 9, 10 + 11, 14 + 15). Note that D_2 experiments will not detect reversible β-H elimination in 2-phenyl-1-butene reductions if the regiochemistry of addition is that depicted in eq 20 (the same H atom is added and abstracted). However, as noted above, D_2 experiments with styrene under vortex mixing conditions gave no evidence for reversible β-H elimination/readdition sequences, which would be implied by C–H/C–D scrambling in the product (products other than ethylbenzene-1,2-d_2).

Origin of Enantioselection. All indications are that enantioselection in the present reactions is "locked-in" in the exothermic, essentially irreversible olefin insertion step (Scheme 4, step i). The absence of major nonlinear effects in rate or ee (*vide supra*) argues against the importance of dimeric species in fixing the stereochemistry (i.e., the k_{-1}/k_1 manifold is not accessed, and k_i and k_{ii} are essentially irreversible), while the temperature dependence of enantioselection (Figure 4) also argues against the interplay of sequential steps in the selecting for product stereochemistry. As discussed above for hydroamination, there are two limiting trajectories possible for olefin approach to and insertion at the monomeric Ln center. The first is a lateral approach. In the most readily visualized scenario, the catalyst (*S*)-epimer affords (*R*)-2-phenylbutane (eq 21) and the (*R*)-epimer affords (*S*)-2-phenylbutane (eq 22). However, exactly

lateral

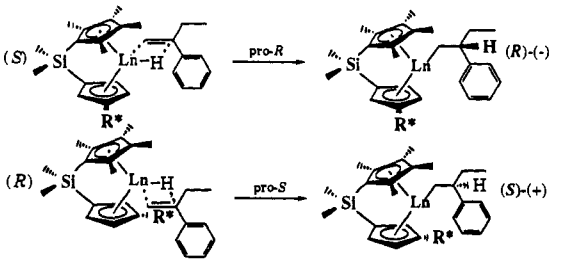

(21)

(22)

the *opposite situation is observed* for the catalytic hydrogenations of 2-phenyl-1-butene and styrene with precatalyst classes **6** and **7**. Alternatively, the frontal trajectory involves central olefin approach along the ring centroid–Ln–ring centroid angle bisector with the bulky phenyl group oriented distal to R* (eqs 23 and 24) and the Ln–H bond bending "back", out of the ring centroid–Ln–ring centroid plane. These same steric arguments apply to the asymmetric deuteration of styrene.

frontal

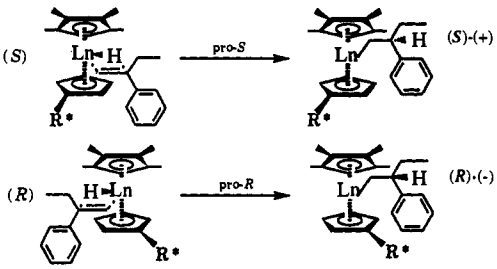

(23)

(24)

The frontal approach has also been suggested for olefin insertion into M–H bonds of tetravalent d^0 $Cp_2MH(X)$ complexes.[45] This trajectory accounts well for the observed stereochemistry of the

(38) (a) Holton, J.; Lappert, M. F.; Scollary, G. R.; Ballard, D. G. H.; Pearce, R.; Atwood, J. L.; Hunter, W. E. *J. Chem. Soc., Chem. Commun.* **1976**, 425–426. (b) Holton, J.; Lappert, M. F.; Ballard, D. G. H.; Atwood, J. L.; Hunter, W. E. *J. Chem. Soc., Dalton Trans.* **1979**, 54–60.

(39) Evans, W. J.; Ulibarri, T. A.; Ziller, J. W. *J. Am. Chem. Soc.* **1990**, *112*, 219–223.

(40) (a) Coughlin, E. B.; Bercaw, J. E. *J. Am. Chem. Soc.* **1992**, *114*, 7606–7607. (b) Coughlin, E. B.; Bercaw, J. E., personal communication.

(41) *Asymmetric Catalysis*; Bosnich, B., Ed., NATO ASI Series E 103; Martinus Nijhoff Publishers: Dordrecht, 1986; Chapter 1.

(42) (a) Nolan, S. P.; Stern, D.; Hedden, D.; Marks, T. J. *ACS Symp. Ser.* **1990**, *428*, 159–174 and references therein. (b) Nolan, S. P.; Stern, D.; Marks, T. J. *J. Am. Chem. Soc.* **1989**, *111*, 7844–7853 and references therein.

(43) (a) Hammond, G. S. *J. Am. Chem. Soc.* **1955**, *77*, 334–338. (b) Lowry, T. H.; Schueller-Richardson, K. *Mechanism and Theory in Organic Chemistry*, 3rd ed.; Harper and Row: New York, 1987; Chapter 2.

present hydrogenation products (Table 2), assuming that the dominant configuration of catalyst present correlates with the dominant product configuration. The rationale rests on the reasonable hypothesis that a bulky olefin preferentially approaches the least sterically-encumbered center of the Cp_2M "wedge" rather than the smaller, more sterically hindered side of the wedge. Molecular mechanics calculations have been performed on the insertion trajectory of norbornene into the U–H bond of $Cp'_2U(H)(OR^*)$ (R^* = [(1*S*)-*endo*]-bornoxide) along the three trajectories (**C**, **D**, and **E**).[44] Pathways **C** and **D** describe approach

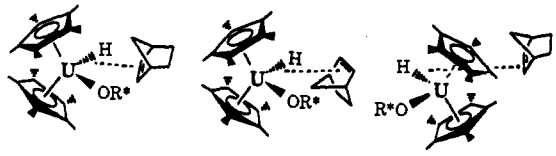

C D E

in the equatorial "girdle" between the U–H and U–OR* vectors, while **E** describes approach from the "side". These calculations reveal that steric impediments to pathway **E** are far larger than those to central trajectories **C** and **D**. Indeed, pathway **C**, which is calculated as the minimum energy trajectory, corresponds to the stereochemically favored course of the insertion reaction. Similar approach arguments rationalize opposite enantioface selectivities for olefin hydrogenation and polymerization catalyzed by chiral ethylenebis(tetrahydro-1-indenyl)zirconocene/methylalumoxane catalysts.[45] Olefin insertion into the reactive Zr–H/R bond should be the stereodifferentiating step for both of these processes (**F**, **G**). The stereochemistry of olefin insertion in

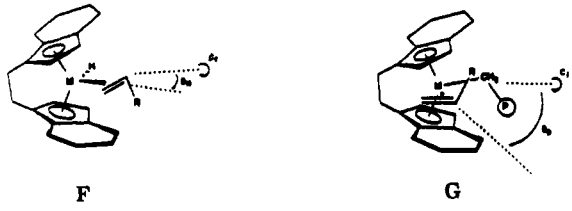

F G

the hydrogenation reaction can be rationalized on the basis of steric interactions incurred in frontal olefin approach, in which acute angle θ_H is formed between the olefin approach vector and the catalyst C_2 axis (**F**). However, for polymerization, the growing polymer chain occupies the central, most open area of the metallocene wedge, where steric interactions are minimized. The incoming olefin must then approach laterally, at an obtuse angle (θ_p) to the C_2 axis of the complex (**G**), resulting in insertion across the opposite enantioface of the prochiral olefin. These results suggest that, in the absence of overriding steric factors, the frontal olefin approach trajectory is the normal mode for olefin insertion reactions of d^0/f^n $Cp_2MH(X)$ complexes.

The present C_1-symmetric organolanthanide complexes are the first class of well-defined, d^0/f^n metallocene-based chiral complexes, not requiring a cocatalyst, which cleanly catalyze the asymmetric hydrogenation of prochiral olefins with high enantioselectivity. Consequently, these systems may be directly characterized with regard to kinetics and mechanism. The actual origin of the molecular enantioselection can be readily rationalized in terms of sterically-based catalyst–substrate interactions. Additionally, the present hydrocarbyl complexes are at least 100× more active than the most active cocatalyzed metallocene reagents and exhibit far higher turnover numbers. The $Me_2SiCp''(R^*Cp)$-LnR catalysts are also more reactive than the parent $(Cp'_2LnH)_2$ complexes, presumably reflecting lessened steric constraints, and are among the most active homogeneous olefin hydrogenation catalysts presently known.

Conclusions

C_1-symmetric $Me_2SiCp''(R^*Cp)Ln$ complexes rapidly and efficiently catalyze the stereoselective hydroamination/cyclization of N-unprotected amino olefins and the asymmetric hydrogenation and deuteration of 2-phenyl-1-butene and styrene under mild conditions with moderate to very high enantioselectivities. Significantly, both antipodes of the products may be prepared by choice of the appropriate precatalyst. For a given chiral auxiliary, one antipode of the precatalyst is significantly more reactive/selective than the other. In addition, the absolute configurations of the precatalysts have been unambiguously assigned from CD spectroscopy and X-ray diffraction studies.[1] Consequently, the stereochemistry of the catalytic products can be rationalized on the basis of presumed catalyst–substrate steric interactions in the transition state of the enantioselective step (operationally irreversible olefin insertion into the Ln–N and Ln–H bond). This investigation also demonstrates the competence of C_1-symmetric complexes in catalytic asymmetric olefin transformations and by inference, in cognate asymmetric transformations[46] and for non-f-metals.[47]

Acknowledgment. We thank NSF for support of this research under Grant CHE9104112. V.P.C. and L.B. thank NSF and Rhône-Poulenc, respectively, for predoctoral fellowships.

(44) Lin, Z.; Marks, T. J. *J. Am. Chem. Soc.* **1990**, *112*, 5515–5525 and references therein.

(45) Waymouth, R.; Pino, P. *J. Am. Chem. Soc.* **1990**, *112*, 4911–4914.

(46) (a) Yamamoto, Y.; Giardello, M. A.; Brard, L.; Marks, T. J., manuscript in preparation. (b) Yamamoto, Y.; Giardello, M. A.; Brard, L.; Marks, T. J. *Abstracts of Papers*, 206th National Meeting of the American Chemical Society, Chicago, IL, August 1993; American Chemical Society: Washington, DC, 1993; INOR461.

(47) (a) Giardello, M. A.; Eisen, M. S.; Stern, C. L.; Marks, T. J., manuscript in preparation. (b) Giardello, M. A.; Eisen, M. S.; Stern, C. L.; Marks, T. J. *J. Am. Chem. Soc.* **1993**, *115*, 3326–3327.